SnowSAR for SnowEx

Year 1 - Snow on

Data delivery report

Reference Code	**:**	MS-NAS-SNX-01N-D06-040
Issue	**:**	4.0
Date	**:**	15th February 2019

MetaSensing BV
Huygensstraat 44
2201DK Noordwijk, The Netherlands
Tel.: +31 71 751 5960
Email: info@metasensing.com

Document Information

Contract Data	
Contract Number:	**FFP Contract Nr. MISTF-008** **(Issued under prime contract Nr. NNG15CR64C)**
Contract Issuer:	**ATA Aerospace, contractor of NASA Goddard Space Flight Center**

External distribution

Name	Organization	Copies
J. Newlin	ATA Aerospace	Electronic
E. Kim	NASA	Electronic

Confidentiality Level		
Unclassified ☐	Restricted ☑	Confidential ☐

Document Status Log

Issue	Change description	Date	Approved
1.0	First version	9th Feb 2017	
1.1	Minor modifications	15th Feb 2017	
2.0	Quality analysis added	10th Jan 2019	
3.0	Appendixes added	22nd Jan 2019	
3.1	Typos and review	28th Jan 2019	
4.0	Approval	15th Feb 2019	

Table of Content

1 Introduction

MetaSensing (MS) is a Dutch company offering radar sensors and services. MS radar products cover a wide range of scientific and commercial applications such as mapping, deformation monitoring, weather forecasting, coastal surveillance, harbor management and more [Ref. 1]. Among the products of MS, the SnowSAR instrument is a simultaneous dual frequency (X and Ku frequency bands) polarimetric radar for snow and ice measurements, developed by MS for the European Space Agency (ESA) and operated during several campaigns worldwide in the past years.

The SnowSAR deployment has been requested by NASA in 2017 in the framework of the SnowEx campaign, a multi-year series of airborne and ground snow missions in US for multi-sensor observations enabling trade studies for snow satellite mission design [Ref. 2]. On behalf of NASA, ATA Aerospace formally requested the service to MS by means of a request for Firm Fixed Price (FFP) quotation [Ref. 3]. Based on the indicated Statement of Work (SoW) a technical proposal has been provided by MS, together with a quotation [Ref. 4]. This has been accepted and the contract for the service has been executed [Ref. 5]. The contract deliverables are defined as:

D1 SnowSAR system preparation (readiness status report)
D2 Installation design (support to the aircraft engineering team and installation document
D3 Successful installation and test flight of SnowSAR instrument on the P3 aircraft
D4 Completion of all scientific flights and uninstallation of SnowSAR from the P3 aircraft
D5 Submission and acceptance of Level 0 and Level 1A SnowSAR data
D6 Submission and acceptance of fully processed data and metadata files, and of final report

The present document represents the contract deliverable D6 of the contract, i.e. the SnowSAR final report. For the snow-on campaign of SnowEx Year 1, the SnowSAR has been installed on board the P-3B Orion Airborne Laboratory platform (P3) by the Scientific Development Squadron One (VXS-1) of the US Navy, during January-February 2017. Previously, an Instrument Readiness Review (IRR) telecon meeting has been held on the 6th of December 2016 among the instruments leads [Ref. 6].

The radar raw data acquired by the SnowSAR instrument during the SnowEx Year 1 camapign have been processed through the MetaSARPro to deliver radiometrically calibrated, geolocated polaimetric SAR images.

Besides this introductory part, the document is organized as follows: chapter 2 describes the main features of the MetaSARPro processing chain; chapter 3 overviews the delivered SnowSAR dataset concerning the SnowEx campaign; chapter 4 provides an assessment of the data quality; some conclusions are drawn in the last chapter; finally, two appendixes at the end of the document describe the NetCDF format of delivered files and the overall acquisitions of the delivered dataset.

2 Data processing

Some insight in the SnowSAR data processing flow is provided in this chapter. The paragraph 2.1 introduces to the MetaSARPro, the processing platform by Metasensing for airborne SAR images generation. The implemented processing steps are detailed in paragraph 2.2.

2.1 The MetaSARPro

As for any other airborne campaign by Metasensing, the collected SnowSAR raw data are processed by means of the MetaSARPro, the airborne SAR software tool by MetaSensing. A screenshot of the MetaSARPro is provided in Figure 1, showing some of its main functionalities. In foreground it is highlighted the window with batch mode set up for efficient handling of multiple datasets.

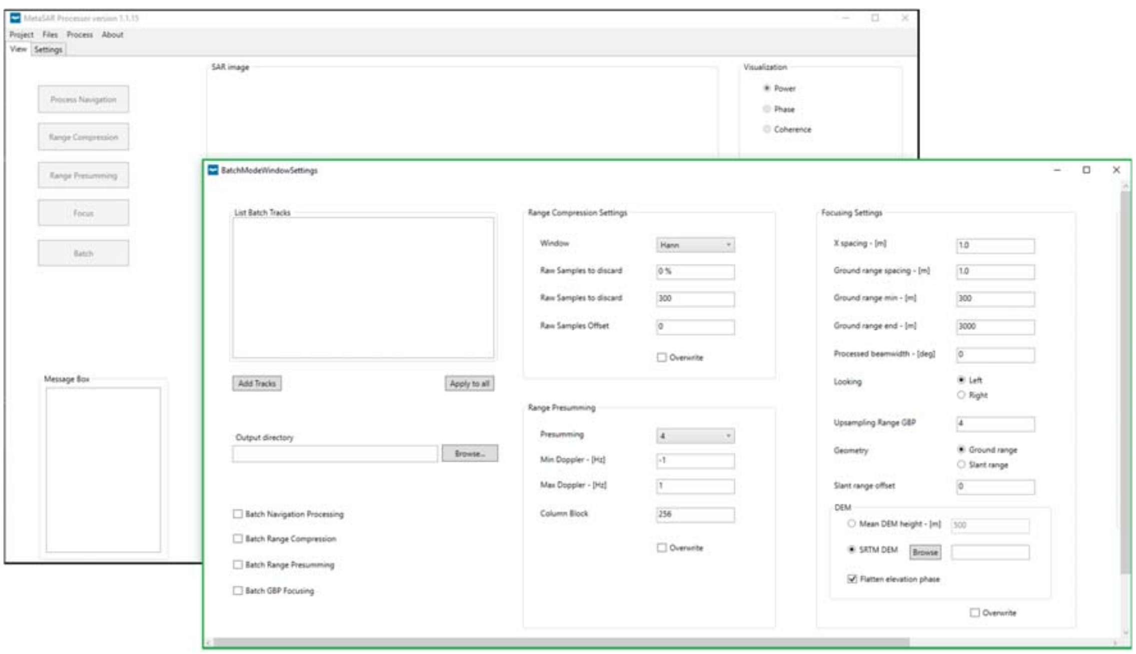

Figure 1 –The MetaSARPro, a SW tool for processing the Metasensing airborne SAR data.

2.2 Processing flow

Figure 2 shows a block diagram for the SnowSAR data processing as implemented by the MetaSARPro to obtain georeferenced, radiometrically calibrated, multi-looked (ML) SAR images (Level 1B) from the collected raw data (Level 0). Each step is detailed in the following sub-sections.

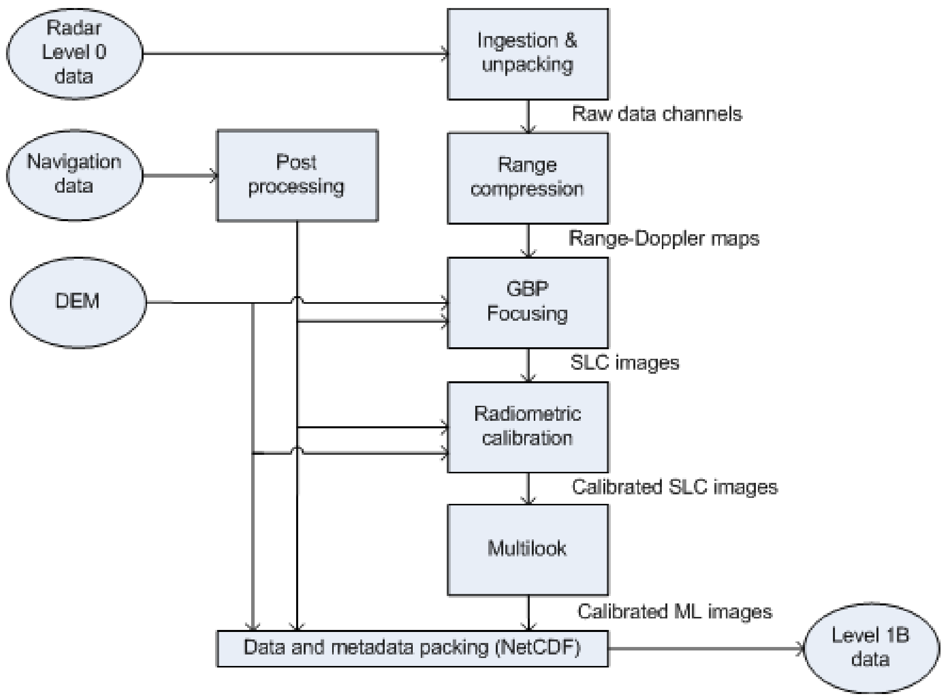

Figure 2 – Block diagram describing the SnowSAR data processing flow.

2.2.1 Raw-data unpacking

As first step, the SnowSAR raw data is ingested and unpacked, i.e., data is grouped according the operational frequency and the polarization channel. This step uses the information contained in the file header. Figure 3 shows the contents of a typical acquisition file from the SnowSAR system, relatively to an acquisition at X-band. The name of the acquisition represents the GPS time in which the acquisition has started. The deramped radar data for all polarimetric channels are stored in fixed-dimensions *.msr* files, whose number depends on the length (in time) of the acquisition. These are joined together during the ingestion phase. Together with radar data, the corresponding configuration file (*.msmpl*) and time synchronization file (*.msmtl*) are provided. A real-time navigation file (*.gps*) is also associated to each acquisition. In general, the GPS file contains both real time navigation information and GPS raw data which can be used during post processing to improve the overall accuracy of the navigation solution.

20170221003652_0.gps	21/02/2017 01:37	GPS File	528 KB
20170221003652_0.msmpl	21/02/2017 01:37	MSMPL File	64 KB
20170221003652_0.msmtl	21/02/2017 01:37	MSMTL File	40 KB
20170221003652_0_1.msr	21/02/2017 01:36	MSR File	20,001 KB
20170221003652_0_2.msr	21/02/2017 01:36	MSR File	20,001 KB
20170221003652_0_3.msr	21/02/2017 01:36	MSR File	20,001 KB
20170221003652_0_4.msr	21/02/2017 01:36	MSR File	20,001 KB
20170221003652_0_5.msr	21/02/2017 01:36	MSR File	20,001 KB
20170221003652_0_6.msr	21/02/2017 01:36	MSR File	20,001 KB
20170221003652_0_7.msr	21/02/2017 01:36	MSR File	20,001 KB
20170221003652_0_8.msr	21/02/2017 01:36	MSR File	20,001 KB
20170221003652_0_9.msr	21/02/2017 01:36	MSR File	20,001 KB
20170221003652_0_10.msr	21/02/2017 01:36	MSR File	20,001 KB
20170221003652_0_11.msr	21/02/2017 01:36	MSR File	20,001 KB

Figure 3: Example of the contents of a SnowSAR acquisition file, relatively to the X-band subsystem. The Ku-band sub-system is characterized by the "_1".

The SnowSAR data extraction is organized in two steps:

- Header extraction.
- Level-0 data extraction.

Using the information included in the header, i.e. instrument configuration and user settings such as used Pulse Repetition Frequency (PRF), Sampling Frequency (F_S), etc, the time-tagged observation data is arranged in a raw-data matrix, one for each receiving channel: rows represent slow time domain, which parametrizes the along track position of the platform (sampled at PRF), while columns represent the fast time domain, which parametrizes the received echoes (sampled at F_S).

2.2.2 Range Compression

Raw data of each channel (deramped frequency-modulated continuous waveforms) are the input for this step. The range compression is implemented as a simple Fast Fourier Transform (FFT) in range. A Hann window is applied before the range compression. Range-Doppler maps are obtained as output of this step, see for example ….

2.2.3 Navigation data post-processing

The SnowSAR system is equipped with a dedicated navigation unit, a compact, single enclosure GNSS+IMU receiver by Novatel [Ref. 7]. The accuracy of the real-time solution is improved during the post-processing by tightly integrating GNSS and IMU solutions, together with differential correction [Ref. 8]. The post-processed navigation solution is used for generating the SAR data and it is provided in the delivered NetCDF files.

2.2.4 GBP Focusing

The SnowSAR processor is based on a time-domain ground-backprojection (GBP) method [Ref. 9], [Ref. 10]. Opposite to any frequency-domain approach, separate motion compensation and range migration correction steps are not required because the GBP algorithm implicitly handles non-ideal motion/sampling and it can precisely perform beam-steering. The GBP algorithm works interpolating and phase correcting each received echo at the desired positions to be focused. Because the radar echo has been sampled according to the Nyquist criterion, it can be interpolated with arbitrary accuracy at any illuminated image position. By coherently adding the contributions of each echo to each desired position, the focusing is performed. The contribution of each echo is computed according to the acquisition geometry.

The GBP algorithm implements the beam steering for the Doppler-filtered range compressed data for each sample on any arbitrary surface grid. The geometry of the output grid can be set to follow any direction: for example, the processed data can be directly projected on the Universal Transverse Mercator (UTM) system. The post-processed navigation information is used to determine the vectors joining the position of the beam center and the position of the point-target in the grid. With the knowledge of the ranges and angles relative to each point-target the vectors are phase compensated and then coherently summed up to form the focused beam. This is repeated for each point-target of the grid. The precise position and attitude information of the aircraft is used in combination with a Digital Elevation Model (DEM). A

90 meters resolution SRTM has been used [Ref. 11]. After GBP focusing step the SAR data comes as Level-1 geo-referenced Single Look Complex (SLC) product in the ground range by azimuth imaging plane (one image per polarization). Each image pixel is represented by a complex (I and Q) magnitude value and therefore contains both amplitude A and phase Φ information.

2.2.5 Radiometric calibration

In the SnowSAR processor the radiometric calibration is implemented to normalize the received power in terms of the antenna radiation pattern and of the flight geometry. Based on the well-known radar equation, the SAR image can be radiometrically calibrated by dividing the power P in each image pixel by a calibration factor K, to give the normalized radar cross-section σ^0[Ref.12]:

$$\sigma^0 = \frac{P}{K(R,\ \theta_{el}\ ,\theta_i)}$$

$$K = \frac{P_t \mathrm{G}_{TX}(\theta_{el})\mathrm{G}_{RX}(\theta_{el})\lambda^2\sigma^0 p_a p_r G_p(R) G_R}{(4\pi)^3 R^4 \sin\theta_i}$$

where,

P_t is the transmitted power,

G_{TX} is the antenna gain (in elevation) for the transmitting antenna,

G_{RX} is the antenna gain (in elevation) for the receiving antenna,

λ is the radar wavelength,

p_a is the along track resolution

p_r is the across track resolution,

G_p is the processing gain,

G_R is the receiver electronic gain,

R is the slant range between target and sensor,

θ_{el} is the antenna elevation angle,

θ_i is the incidence angle.

The flight geometry (slant range R and incidence angle θ_i) is obtained thorough the post-processed navigation data and DEM information. The antenna radiation patterns have been measured in an anechoic chamber and together with the flight geometry are used to estimate the antenna gain for each antenna pointing direction (in elevation). This operation is performed for all polarization combinations.

The calibration factor is derived by measuring the SAR system against reference point targets with well-known radar cross section. To this extent, eight corner reflectors were provided for deploying over the acquisition sites. The locations of the corners can be identified within a SAR image; their reflectivity values are used to normalize the image reflectivity per unit area (σ_0).

2.2.6 Multilooking

To reduce the inherent speckle noise of radar images, either spatial filtering or multi-look processing can be applied, both at the expense of spatial resolution. The SnowSAR processor implements the multi-looking method. Figure 4 shows the basic principle. The radar beam is divided into several sub-aperture (three in the figure), each one providing an independent "look" at the illuminated scene. The final output image is obtained by summing and averaging together the output of each look, in which the amount of speckle is reduced.

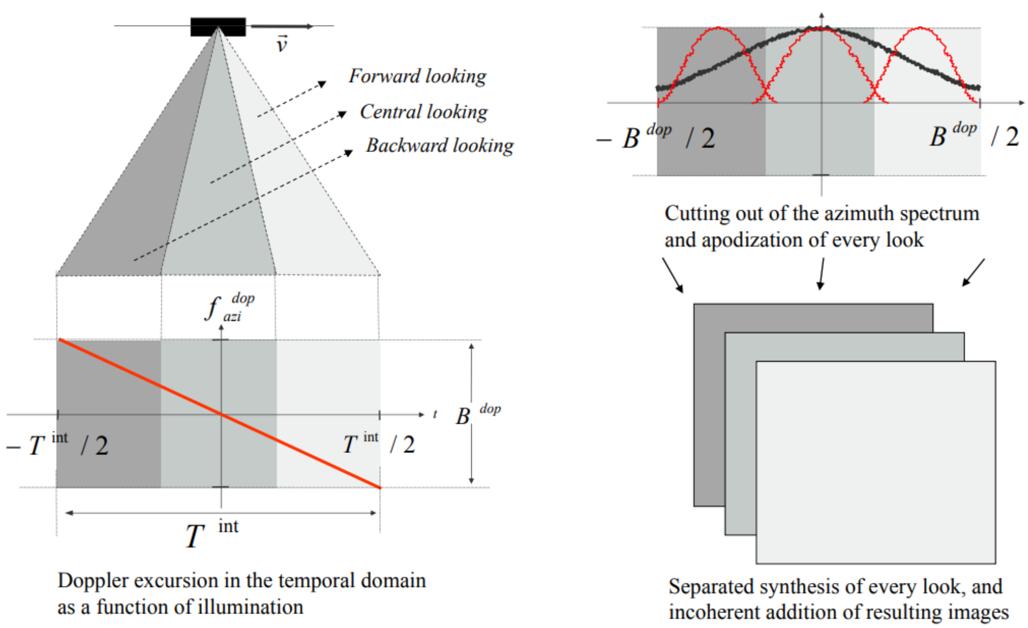

Figure 4: Principle of multi-look processing [Ref. 13].

The implemented number of looks depends on the processable Doppler bandwidth, which can vary from day to day based on the acquisition conditions (AC ground speed, wind, etc..).

As an example, based on the acquired data during the 21st of February over the Gran Mesa site,. the SnowSAR processor has been configured with 9 looks overlapping at 50% with each other, resulting in an equivalent number of 4.5 looks with an image resolution of 1m x 1m.

In general, information about the number of looks of the delivered images is given within the NetCDF file.

2.2.7 NetCDF Encapsulation

The final step of the SnowSAR processing chain is represented by the NetCDF encapsulation of the processed data and of all the relevant ancillary data such as timing tags, geographical position, radar/processing parameters, etc. This kind of format is widely used for array-oriented scientific data representation. A detailed description of the contents of the delivered SnowSAR data in NetCDF format is provided the Appendix A of this document.

3 Delivered data

The SnowSAR data products within the first year of the SnowEx project consist of radiometrically calibrated Level-1 multilooked data and are delivered together with the available metadata. The provided SAR image resolution is 1 meter x 1 meter. Data have been acquired in a standard stripmap imaging method and in full polarization mode (VV, VH, HV, HH). However, as shown in the next chapter, some polarization channels show very low performance.

Each acquisition track is delivered in the following formats:

1) NetCDF files, see Appendix A
2) Geotiff of 32 bits of each SAR image
3) Geotiff of 8 bits (scaled form -33 dB to -3 dB) for quick visualization.

The delivered data are summarized below.

Table 1 – Overview of delivered SnowSAR data

Date (local)	Nr. of images	Frequency band	Notes
16th /2	3	X, Ku	First actual check flight of SnowSAR on P3
18th /2	9	X	Technical issue at Ku band subsytem
21st /2	21	X, Ku	Bad weaher conditions (high wind tourbolence)
22nd /2	2	X, Ku	Bad weaher conditions (high wind tourbolence) and new techincal issue at the instrument.

The complete list of the delivered data is written in the Appendix B of this document.

4 Data quality

4.1 Navigation data

Navigation data is acquired by a GNSS/IMU system integrated in the SnowSAR instrument, namely a SPAN-CPT unit by Novatel [Ref. 7]. To improve the accuracy of the real-time computed solution, a post-processing software tool has been used for tightly coupling the GNSS and IMU data and for correcting data with ground base information.

As an example of the achievable navigation data performance, the trajectory flown during the 21st of February 2017 is here discussed. Figure 5 shows the postprocessed data resulting in the overall trajectory. Highlighted in white the actual SnowSAR acquisitions can be spotted out, performed on the Senator Beck site (unique acquisition at the top of the figure) and on the Gran Mesa site (repeat acquisitions at the left-hand side of the figure).

The estimated accuracies of the computed position and attitude solutions are given in Figure 6 and in Figure 7; on the top part of both the plots, the time slots in which SnowSAR data have been actually acquired are highlighted in red. Overall statistics are provided in Figure 8.

Figure 5: Trajectory flown during the 21st of February 2017. In white the actual SnowSAR acquisitions

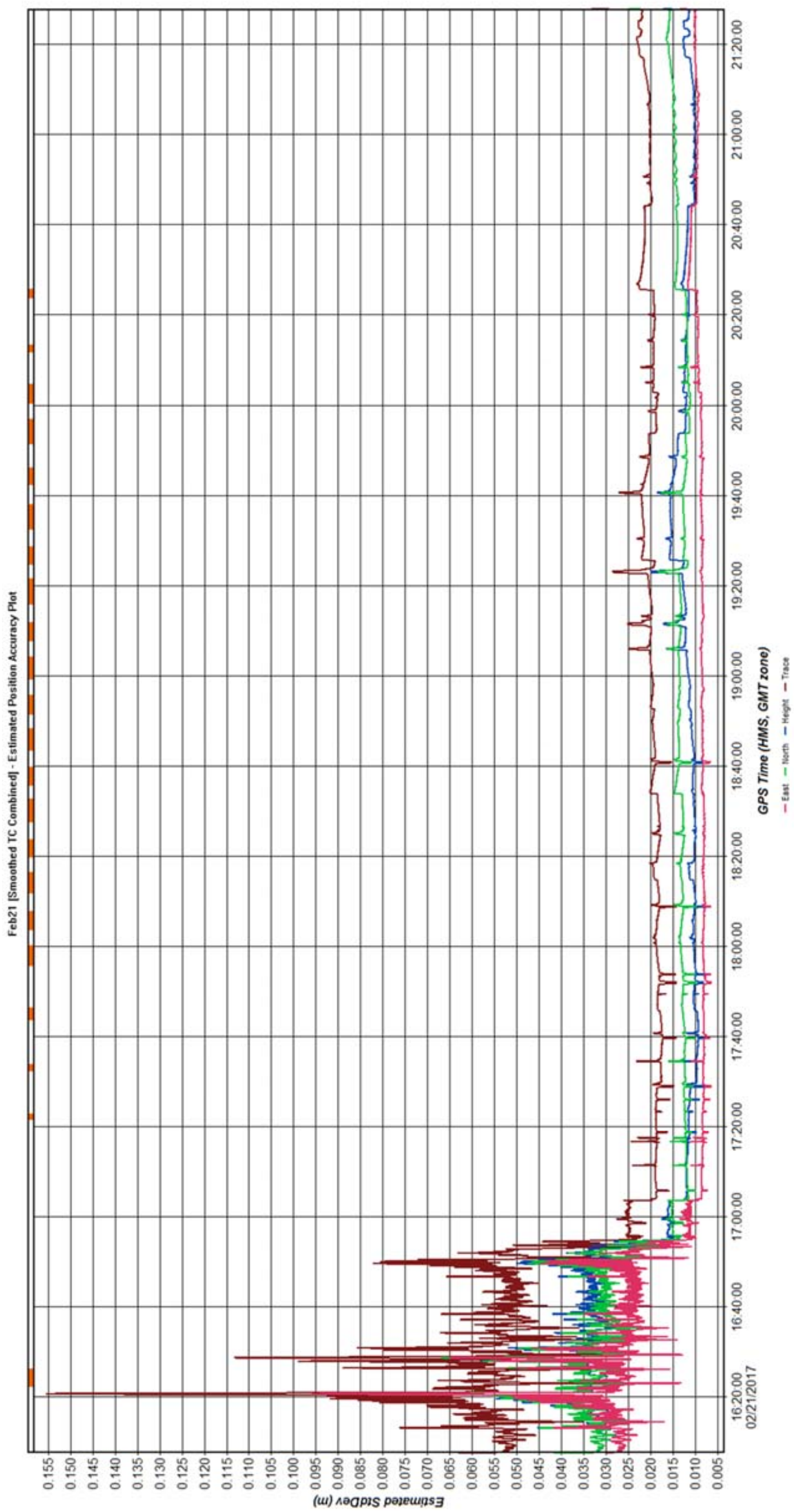

Figure 6: Position accuracy (estimated standard deviation) as a function of time for the postprocessed navigation solution, flight of the 21st of February 2017.

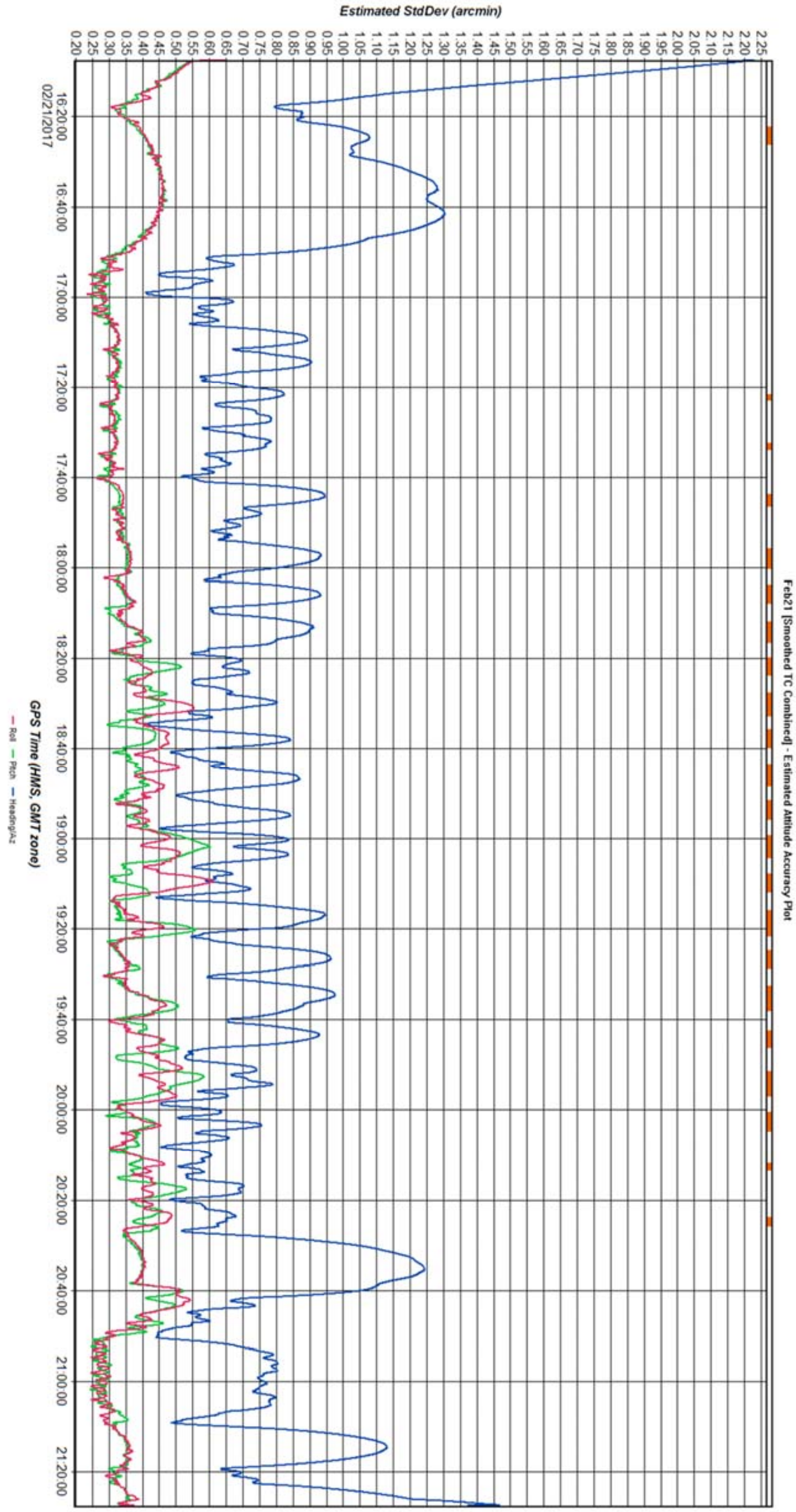

Figure 7: Attitude accuracy (estimated standard deviation) as a function of time for the postprocessed navigation solution, flight of the 21st of February 2017.

Feb21 [Smoothed TC Combined] - Estimated Position Accuracy P...

Time range:
Start: 230856.0 1937 16:07:36.0 02/21/2017
End: 250075.0 1937 21:27:55.0 02/21/2017

Stat	East	North	Height	Trace
Rms:	0.0140	0.0181	0.0175	0.0288
Avg:	0.0118	0.0163	0.0152	0.0252
Max:	0.0957	0.0901	0.0830	0.1554
Min:	0.0065	0.0097	0.0076	0.0143

Feb21 [Smoothed TC Combined] - Estimated Attitude Accuracy P...

Time range:
Start: 230856.0 1937 16:07:36.0 02/21/2017
End: 250075.0 1937 21:27:55.0 02/21/2017

Stat	Roll	Pitch	Heading/
Rms:	0.3843	0.3786	0.8356
Avg:	0.3783	0.3725	0.7966
Max:	0.6511	0.6468	2.2280
Min:	0.2340	0.2421	0.4061

Figure 8: Statistics of the accuracies of the navigation solution computed flight performed on the 21st of February 2017. Left: position [m]; right, attitude [arcmin].

Generally, a reasonably good accuracy (cm-level) in the single position estimation (East, North, Height) is reached, resulting in an overall trace accuracy of less than 3 cm. The attitude accuracy estimation is also satisfactory, with roll and pitch measurement accuracies better than 0.4 arcmin (0.006°), while the heading accuracy (typically less precise than the other two) is better than 1° arcmin (0.017°). Similar navigation performances are achieved for the SnowSAR flights in other days of the SnowEx year 1 mission.

After the overall flight is postprocessed, the navigation data relative to each acquisition is extracted and saved for SAR processing. An example is shown in Figure 9, where different parameters are plotted as a function of time for a track on the 21st, showing quite some turbulent conditions. Variation of roll and pitch angles exceeding 10° within the acquisition can be noticed.

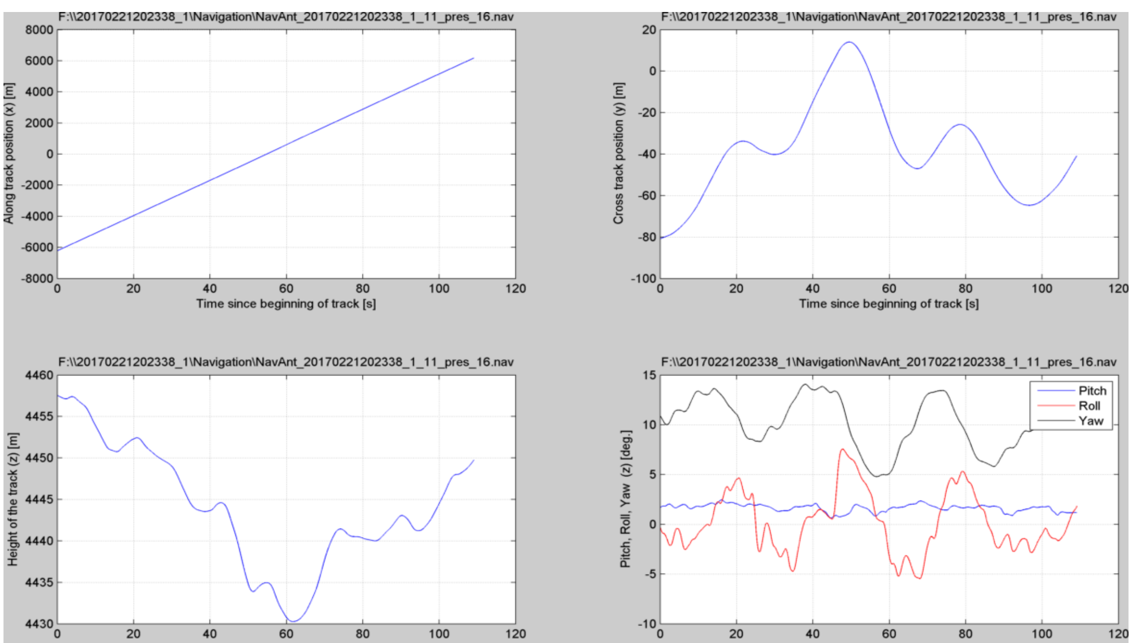

Figure 9: Navigation data for SnowSAR acquisition 20170221202338.

4.2 Range-Doppler maps

After the range compression step the radar data can be visualized in terms of Range-Doppler (RD) maps: this gives a direct feedback of the data quality with respect to SAR processing. For example, it is possible to estimate the noise floor level and the signal power, thus the SNR; additionally, it is possible to check the clutter coverage on ground, the processable Doppler bandwidth and the Doppler centroid variations.

Figure 10 shows RD maps of data acquired at X-band during February 21st, 2017 (acq. 20170221202338) for the four polarimetric channels; (a) and (b) indicates two different moments of the acquisition. For each one of these, clock-wise from top left there are HV (11), HH (12), VH (22) and VV (21) channels, where the first and second letter are related to the transmitter and receiver channels, respectively. Similarly, Figure 11 shows RD maps of data acquired at Ku band in the same timeframe.

From the plots, the cross-pol channels show lower clutter returns with respect to the co-pol channels. This is quite usual in SAR measurements. However, a higher noise level can be noticed in some channels with respect to others, those where H-pol is involved. This is an unusual feature. The cause of this lower performance is not clear, and it is presumably due to a sub-optimal installation, with the RF antenna interacting with the surrounding elements in the radome.

By comparing the Range-Doppler maps (a) and (b) within the same acquisition track an evident variation in the SNR can be observed, due to attitude variation of the aircraft during measurements (see Figure 9). As an example, the SnowSAR antenna radiation patterns for the V pol are plotted in Figure 12, to show the narrow main lobe in the azimuth direction: the 3dB beamwitdh is ~5° and 4° for X- and Ku-band, respectively. This means that, for an optimal SAR processing, the yaw attitude variation of the aircraft during measurements should have not exceeded ±2°, in order to uniformly illuminated the scene for a enough time. Unfortunately, weather conditions were not collaborating during the whole campaign, with the result of quite unstable flights. Negative consequences are derived in the final processed SAR images in terms of loss of resolution and calibration quality.

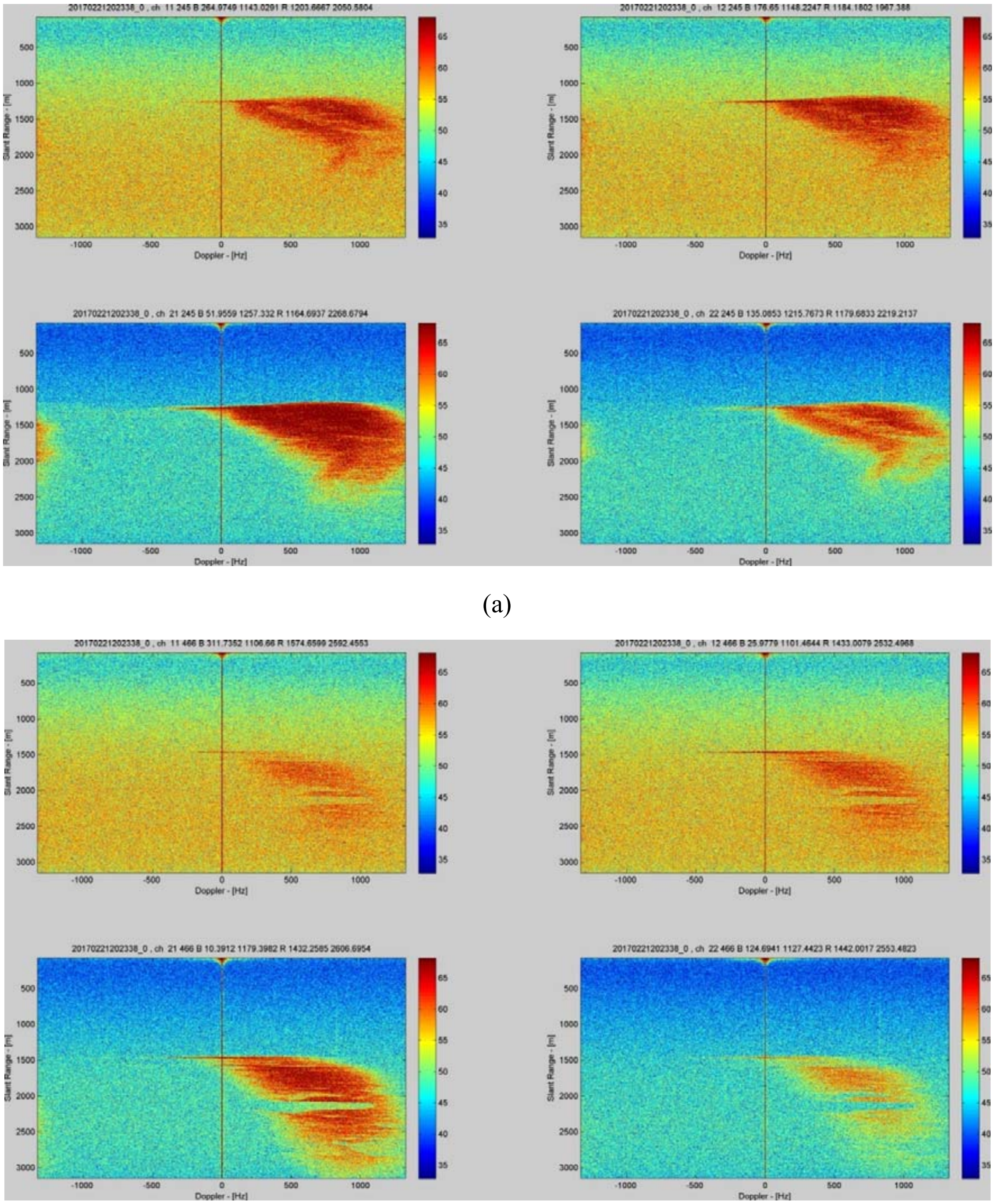

(a)

(b)

Figure 10: – Example of RD maps processed at X band for acquisition 20170221202338, where (a) and (b) show the RD map two different moments of the acquisition. For each (a) and (b) figure, clock-wise from top left there are HV (11), HH (12), VH (22) and VV (21) channels,

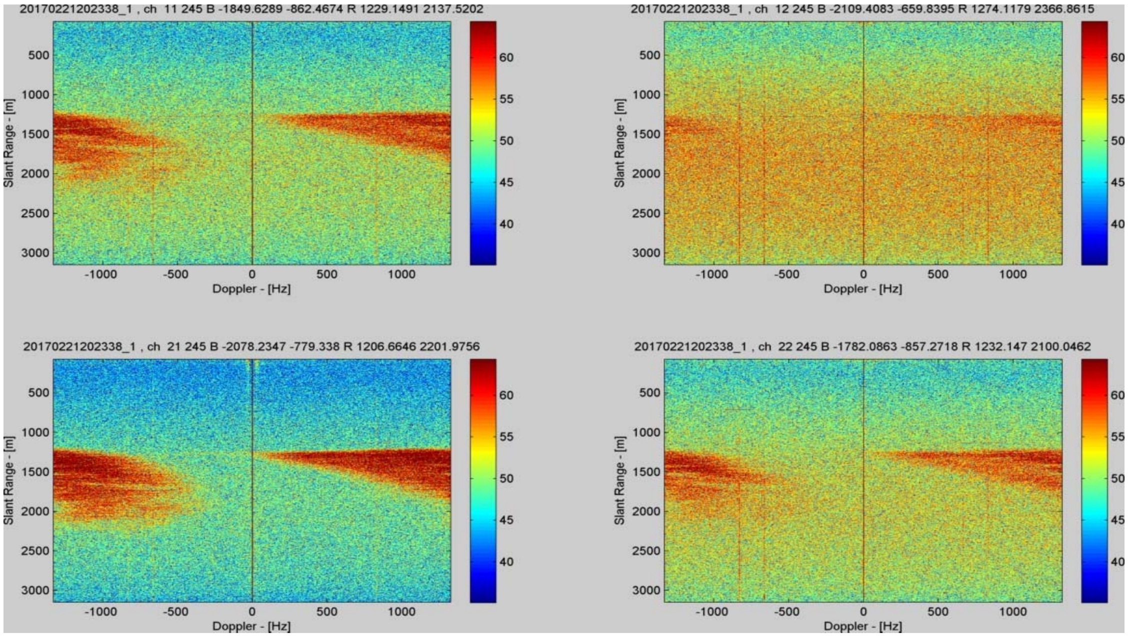

(a)

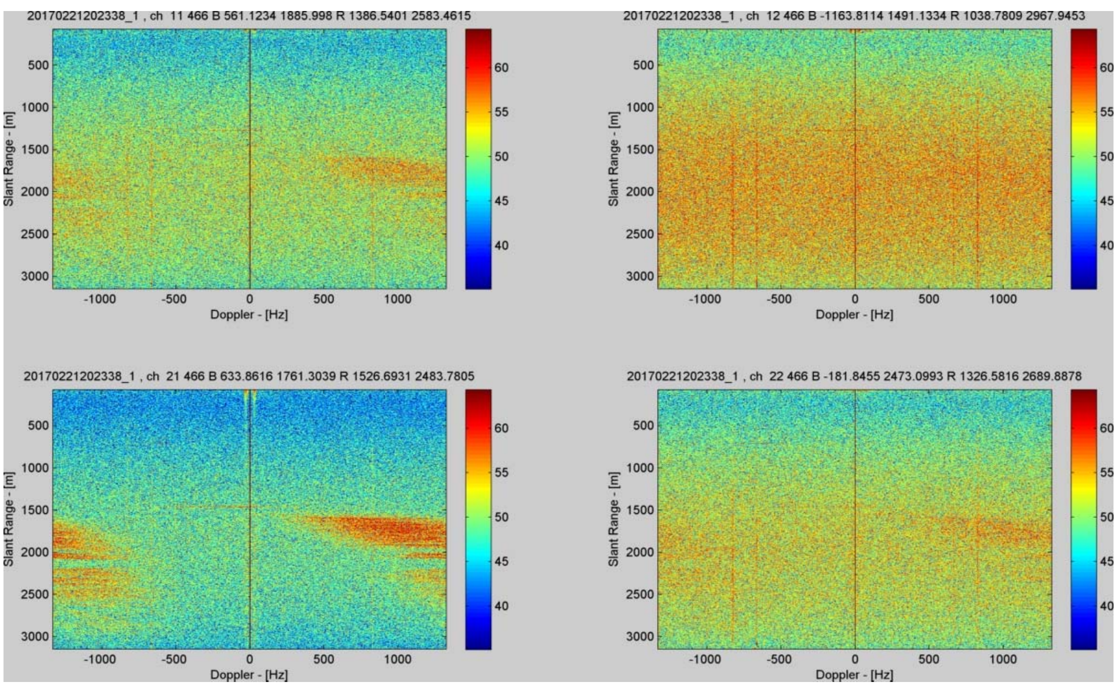

(b)

Figure 11: – Example of RD maps processed at Ku band for acquisition 20170221202338, where (a) and (b) show the RD map two different moments of the acquisition. For each (a) and (b) figure, clock-wise from top left there are HV (11), HH (12), VH (22) and VV (21) channels,

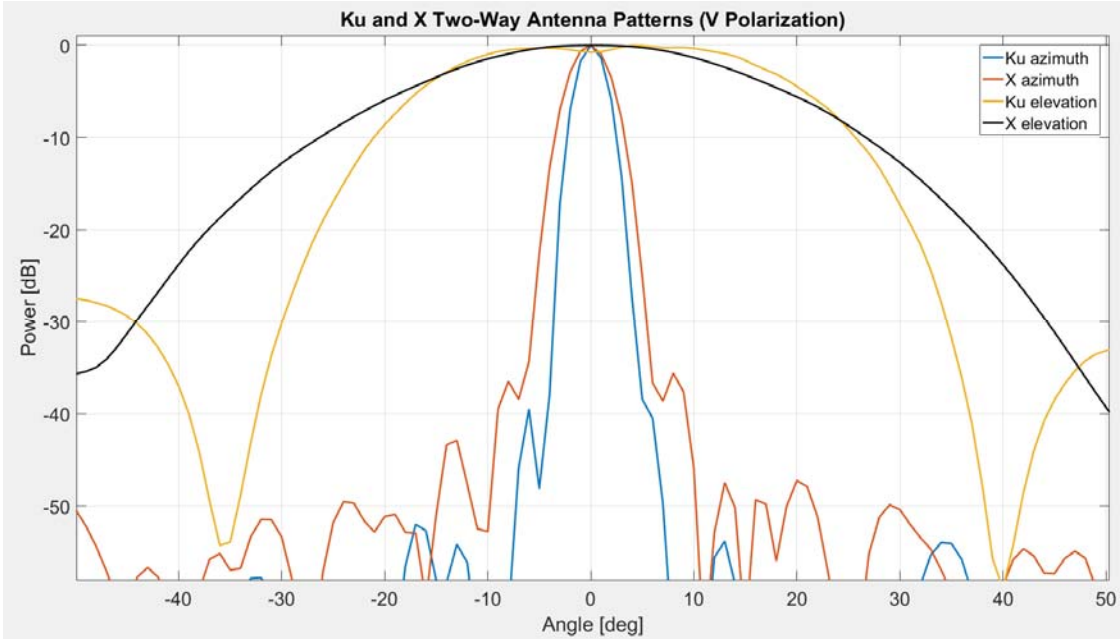

Figure 12 – Antenna radiation patterns at V-polarization (two-way).

4.3 SAR Images

As an example, calibrated ML (9 looks with 50% overlapping) SnowSAR geotiff images (track number 20170221202338) at X- and Ku-band are imposed over a google earth image in Figure 13 and Figure 14, respectively.

The black areas at the border of the strip images represent dummy values, to mask out the areas where the antenna pointing is far from the designed direction. Due to the high roll variations of the aircraft during the acquisitions, sometimes significant part of the images is masked out, especially at Ku-band because of the more directive radiation pattern in elevation. As expected from the discussion of the previous paragraphs of this chapter, the best images are the VV ones, because of the highest SNR.

4.3.1 Corners deployment

The SAR images shown in Figure 13 and Figure 14 were acquired along the designed track with the corner reflectors. Six of them were deployed on top of the frozen Island lake. *Table 2* provides the geographical positions and tilting angles of the corners. Their position and orientation were designed to be optimally seen across the image swath for an acquisition altitude of 6500 ft AGL. However, due to weather conditions, the same track has been performed at an altitude of 4000 ft AGL. For this reason, only 4 corners are visible in the processed images, two the two at shorter ranges (CR5 and CR6) fall out of the antenna beams.

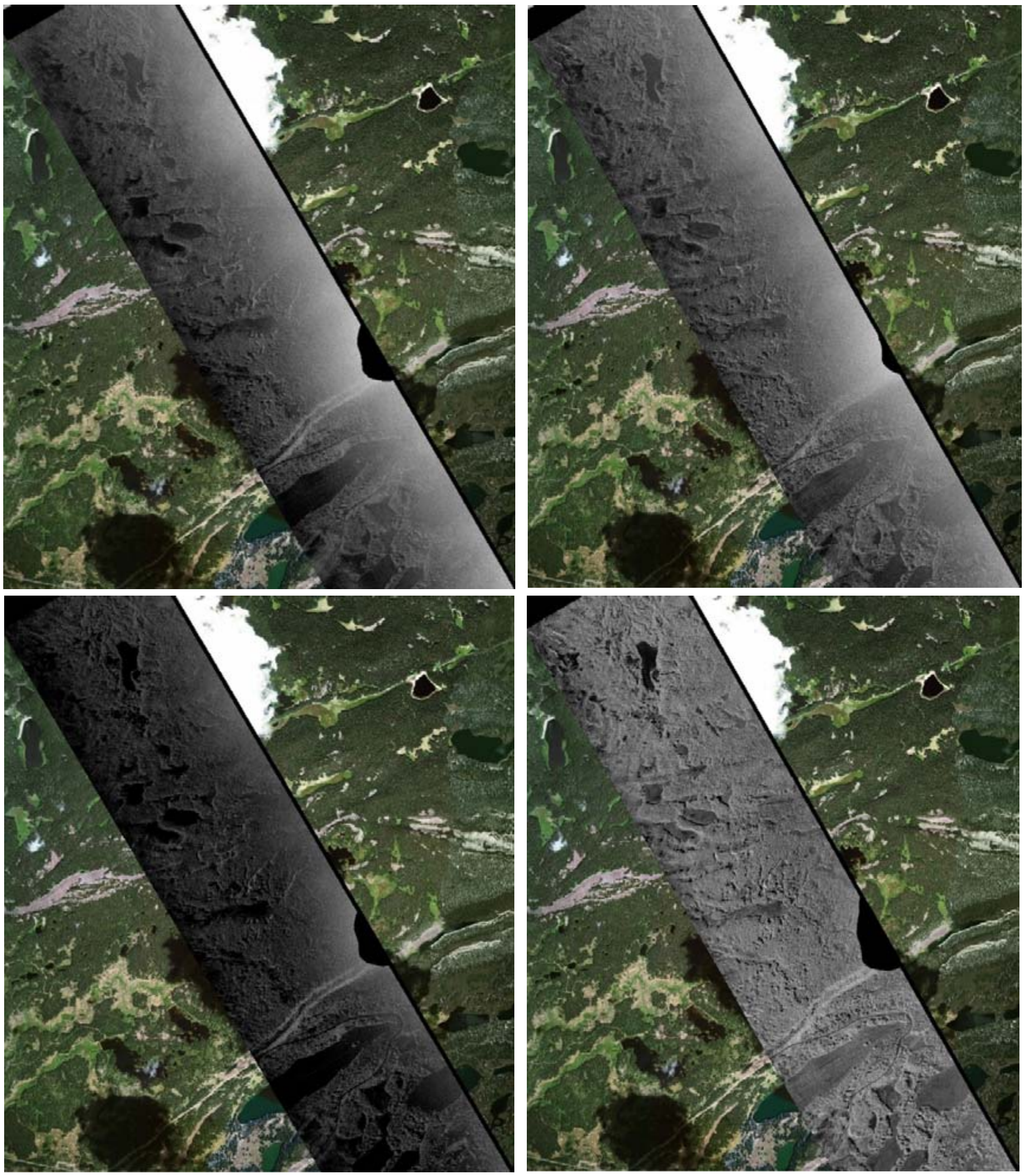

Figure 13 - SnowSAR images at X band, relatively to the track 20170221202338. From top left, clockwise: HV, HH, VV, VH polarizations. Geotiff format, intensity values scaled from -30 to 0 dB.

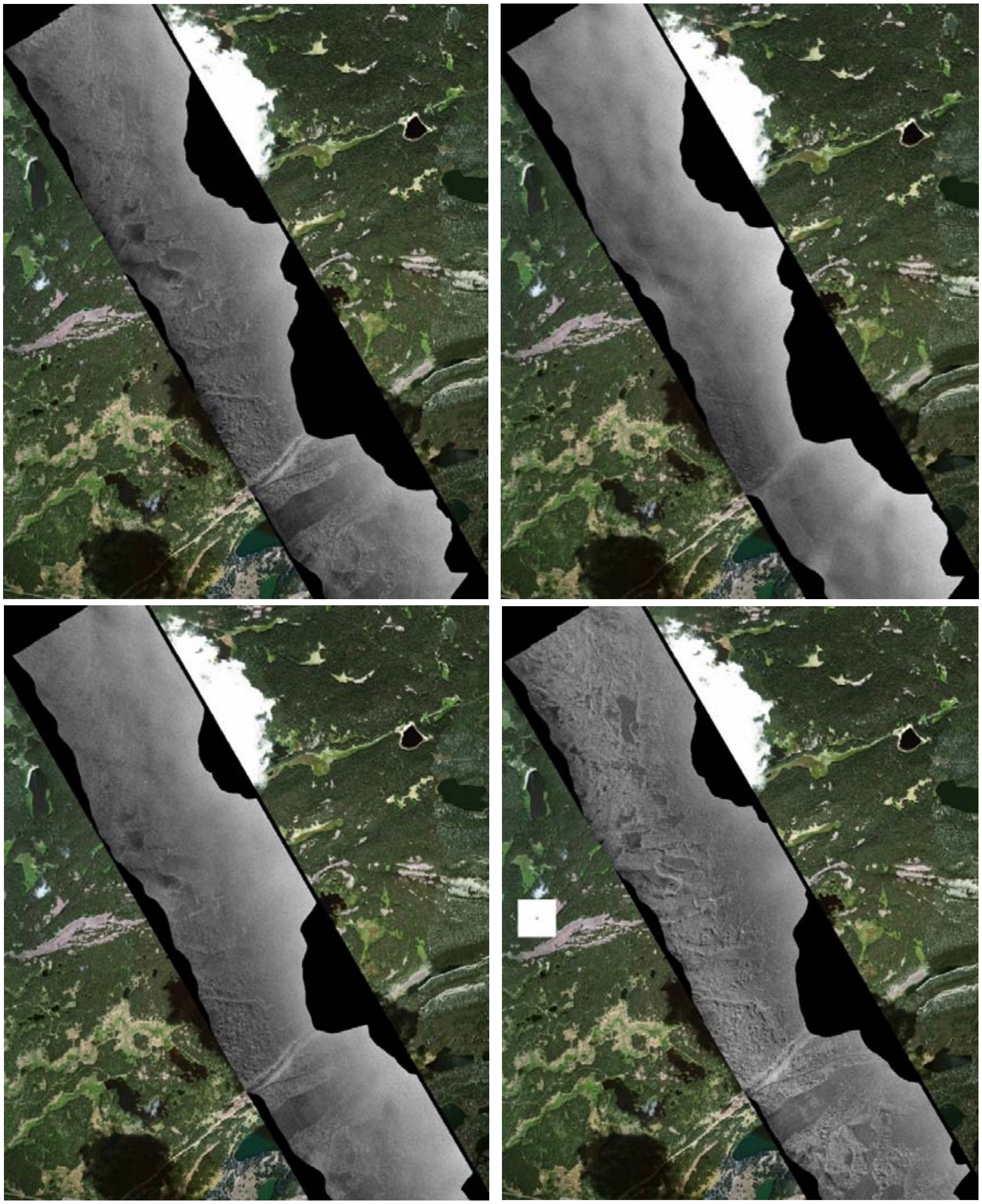

Figure 14 - SnowSAR images at Ku band, relatively to the track 20170221202338. From top left, clockwise: HV, HH, VV, VH polarizations. Geotiff format, intensity values scaled from -30 to 0 dB.

Table 2 – Measured geographical position and tilting angle of corner reflectors during the SnowSAR acquisitions

CR#	Latitude	Longitude	Tilt angle [°]
1	39.038648	-108.002	5
2	39.037122	-107.99911	5
3	39.039106	-107.99622	-5
4	39.04028	-107.99333	-15
5	39.03306	-108.00778	35
6	39.034324	-108.00489	25

Figure 15: designed *corner reflectors positions over the Island lake at the gran Mesa site, as summarized in Table 2.*

CR1, CR2 and CR3 are visible in the processed co-pol SAR images, as shown by the red circles in Figure 14. The response of CR4 is very weak and it is not visible in the image. Therefore, only 3 corners can be used for calibration purposes. From the processed SAR image CR1 results in a different position w.r.t. what reported in Table 2. Most likely the corner was moved from its original location due to operational reasons, without the new position to be logged again. CR1, CR2 and CR3 appear in the SAR image under a look angle of 29°, 31° and 40°, respectively.

(a)

(b)

Figure 16: Corner reflectors visible in the red circles of processed SAR images (VV) at (a) X-band and at (b) Ku-band.

4.3.2 Geometric calibration performance

During the 21st of February for three times SnowSAR data have been acquired along the track with the corner reflectors. The processed images 20170221202338, 20170221201129 and 20170221173206 are used to build a statistic. As explained in the previous paragraph 4.3.1, the positions of only 2 corners can be used for the estimation of the accuracy of the geometric calibration, so finally 6 observations can be used to build up the statistic.

As an example, Figure 16 shows a detail of the corner reflector C3 within georeferenced SnowSAR images at X- and Ku-band. The red cross represents the measured GPS position (from Table 2). This has been repeated for each image available, and similar images have been also generated also for the other corner C2.

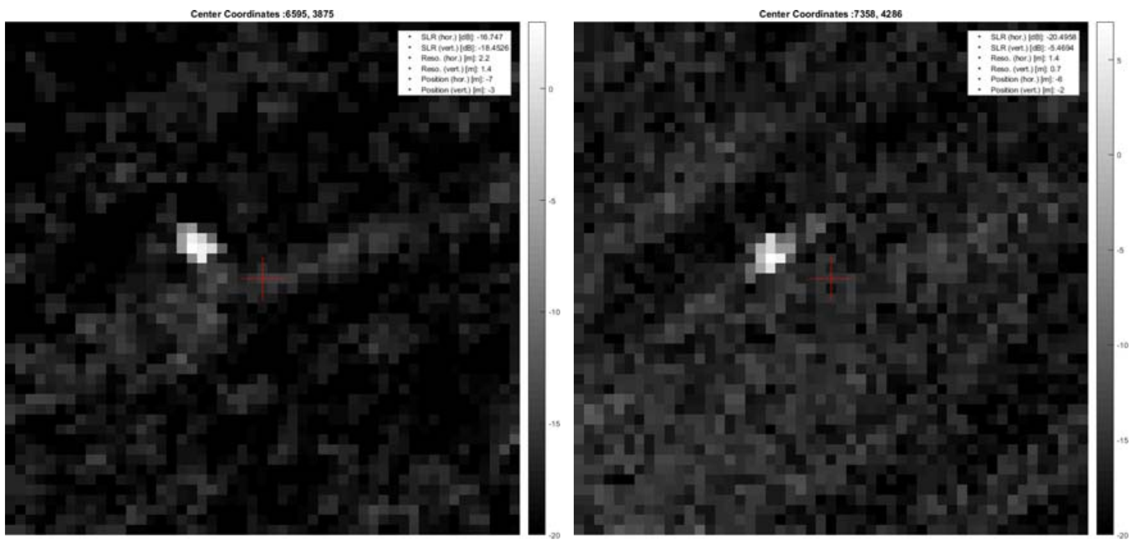

Figure 17: Detail of the corner reflector C3 on X- (left) and Ku-band (right) SAR georeferenced images (VV). The red cross indicates the position of the corner as it has been measured on the field.

The *absolute* geometric accuracy is estimated as the Root Mean Square (RMS) of the distances between the position of the brightest pixel of each corner in the georeferenced SAR image (UTM coordinates) and the position logged in the field by a GPS receiver. The *relative* accuracy is the standard deviation of these distances. The estimated accuracies of the geometric calibration are given in Table 3.

The relative accuracy is a consequence of the image shifts caused by residual motion errors, typically ranging between 1 m to 3 m in along track direction in optimal conditions. However, in turbulent flights as the one here discussed, the deviation can be even more. In the analyzed data this appears mainly in North direction, because the calibration tracks are flown in North-South direction. The contribution of inaccuracy of the measuring GPS device should be also considered in the provided estimations.

Table 3 – Estimated position accuracy [m] of georeferenced SnowSAR images.

Frequency band	Absolute (RMS)			Relative		
	East	North	Norm.	East, North, Norm.		
X	5.1	6.7	8.4	2.4	6.5	6.9
Ku	4.9	6.9	8.5	2.0	6.6	6.9

4.3.3 Radiometric calibration performance

The required absolute calibration factor is derived by measuring the SAR system against reference point targets with well-known radar cross section, i.e. the corner reflectors. These were deployed by ground teams before the acquisition flights.

Figure 18: Square trihedral corner reflector being deployed on the field by ground team.

Figure 20 to Figure 22show the Impulse Response Function (IRF) for the four corners C1-C4, at the two frequency bands and for all polarization channels, relatively to the SAR image 20170221202338, for both azimuth and range directions.

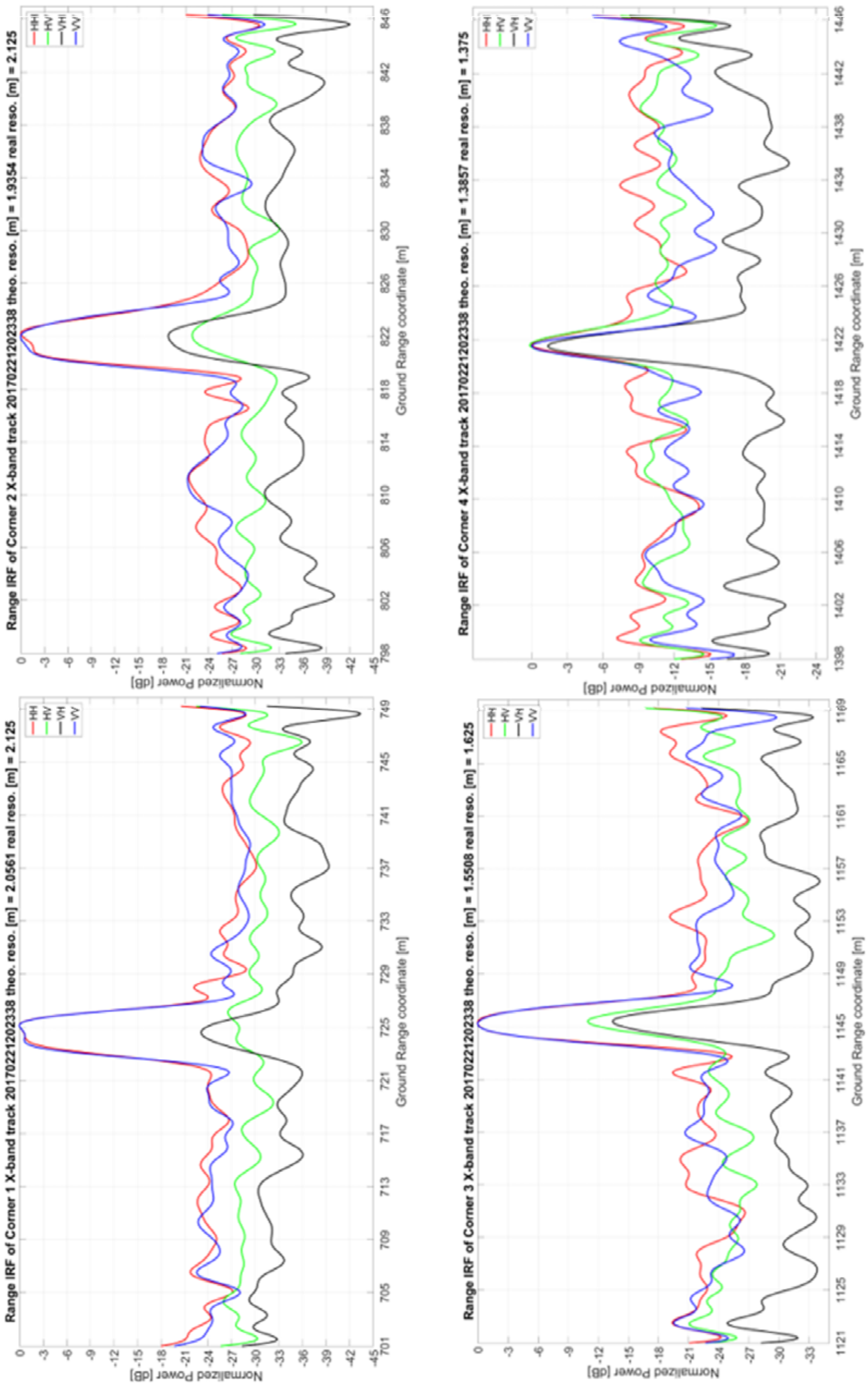

Figure 19: Range IRF at X band for the four corners and for the different polarization schemes, relatively to the SAR image processed form dataset 20170221202338.

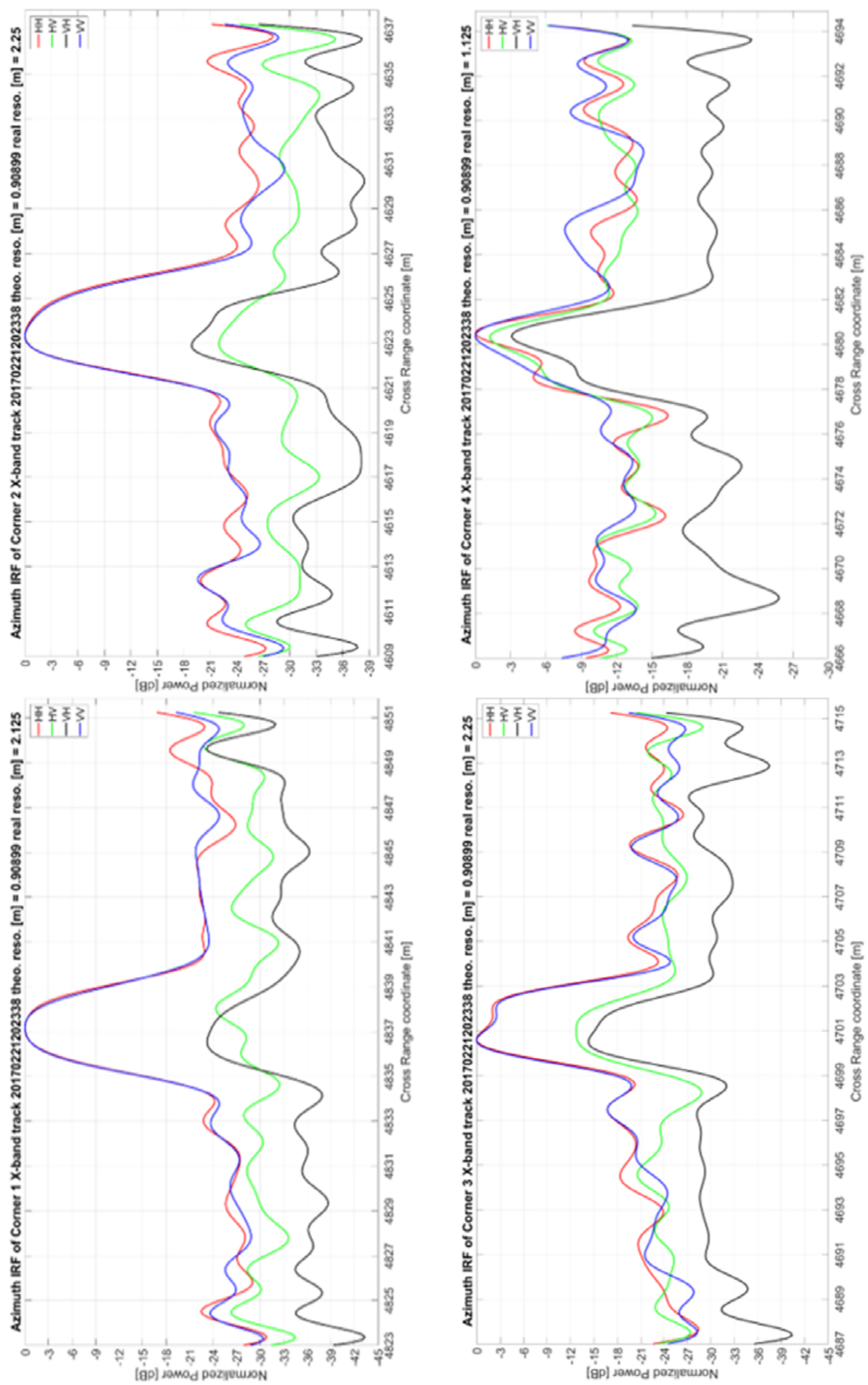

Figure 20: Azimuth IRF at X band for the four corners and for the different polarization schemes, relatively to the SAR image processed form dataset 20170221202338.

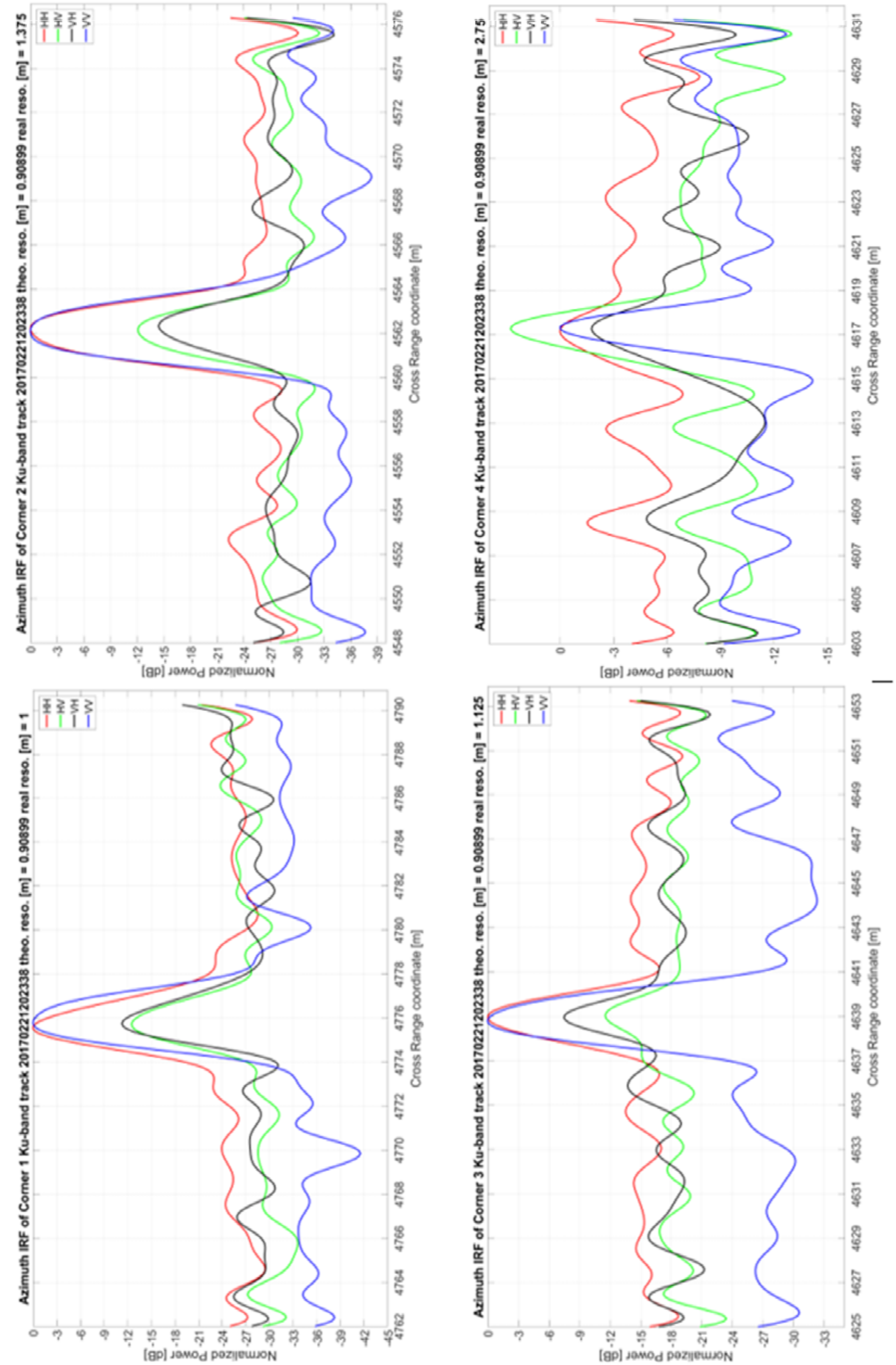

Figure 21: Azimuth IRF at Ku band for the four corners and for the different polarization schemes, relatively to the SAR image processed form dataset 20170221202338.

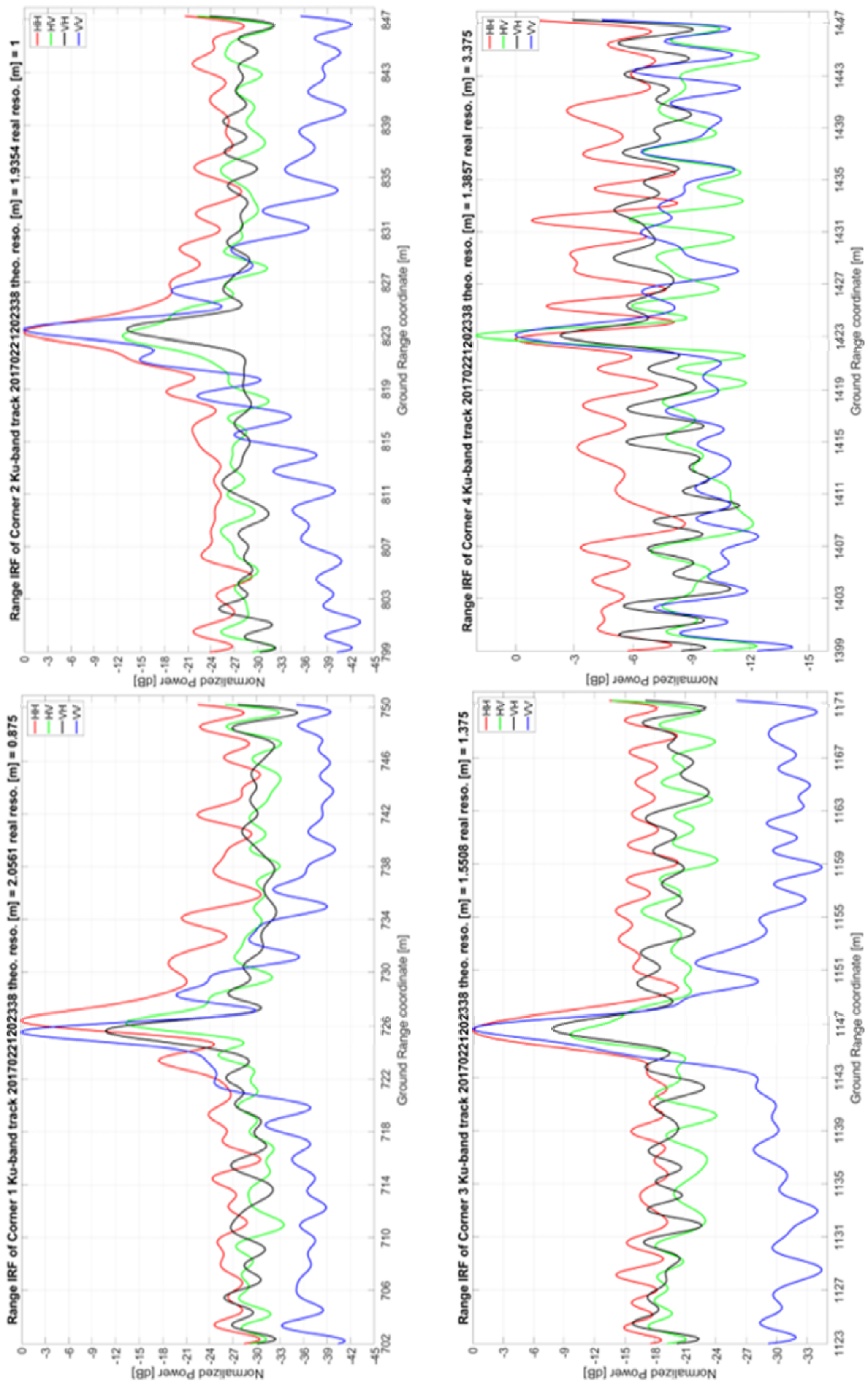

Figure 22: Range IRF at Ku band for the four corners and for the different polarization schemes, relatively to the SAR image processed form dataset 20170221202338.

CR4 is not well visible in the SAR images, so the geographical position which was logged in the field is here used to localize it. In general, from the IRF analysis CR1 and CR2 show plots matching the theoretical expectation and with the polarization response is in accordance with the antenna characterization. CR3 shows lower SNR and the polarizations are not so well defined. CR4 results in a very weak response and the polarization response is not reliable at all. Presumably CR3 and CR4 underperform due to some un-optimal alignment. Therefore, for the estimation of the radiometric accuracy only CR1 and CR2 can be considered, because of their reliable IRF performing as expected at all polarizations.

Only two tracks out of three can be used for the analysis, -202338 and -201129: during these acquisitions the corners were illuminated under similar angle by the RF antennas, while in the -173206 there is 8° difference in the illuminated direction to the corners, due to the roll of the aircraft. Eventually, only 4 observations for each frequency band are available to build out a statistic about radiometric accuracy.

The absolute radiometric accuracy is estimated as the RMS of the differences between the theoretical RCS of the corner at the considered frequency and the RCS values read from the corners within the calibrated SnowSAR images. The square trihedral corners had side length of 30 cm (see Figure 18) resulting in a RCS of 25.3 dB and 30 dB at X- and Ku-band, respectively. The relative accuracy is estimated as the standard deviation of these differences. If the SAR images are slightly defocused, rather than relying in the only peak value of the images, the integral method is used [Ref. 14]. Table 4 summarizes the radiometric calibration accuracy for SnowSAR measurements of the 21st of February.

Table 4 – Radiometric accuracy for measurements		
Radiometric accuracy	Absolute (rms)	Relative (std)
X-band	3.46 dB	1.89 dB
Ku-band	3.22 dB	2.45 dB

5 Conclusions

This document represents the deliverable D6, i.e. the final report, of the contract between MetaSensing BV and ATA Aerospace for the use of SnowSAR instrument during the SnowEx campaign [Ref. 5]. The document is associated to the submission of fully processed data and metadata files, together representing the fourth and last milestone of the project.

Besides for an introductory part, the general processing flow leading to the delivered data is discussed. Data quality analysis is provided for reference. Unfortunately, the campaign execution has been thwarted by several factors, including technical issues and adverse weather conditions. This is the reason for which during the campaign a low amount of SnowSAR data has been successfully acquired with respect to expectations. Also, data quality has been negatively affected by the not optimal preparation phase: any test flight has been possible prior to the campaign and during the science flights some issues have been found out, presumably caused by the interaction between system and surrounding elements, including the protecting radome. This last is supposed to be the cause for the lower SNR achieved with the H-pol signals. From the data collection point of view, the most advantageous day of the campaign has been the 21st of February, in which the SnowSAR sub-systems worked properly during the whole day. However, due to poor weather conditions, the flight has been quite unstable, with evident consequences in the overall SAR data quality. Negative consequences can be seen in the obtained SAR image focusing quality, i.e. by the resolutions and radiometric performance shown by the analysis on the corner reflectors. It should be noted, however, that the very limited number of available observations limits the statistical value of the results.

A quantitative uncertainty for the geometric and radiometric calibration is derived based on the corner reflectors in the SAR images. Three corner reflectors have been used to geometrically and radiometrically characterize the SnowSAR products. The overall absolute geometric accuracy of the geo-referenced SAR data is ~8.5m. The overall (averaged between X and Ku) absolute radiometric is 3.3dB and the relative accuracy is 2.2dB. The main sources of error in the radiometric calibration can be found in the fluctuations of the RF antenna coverage on the ground due to the weather-related strong attitude variations of the aircraft during the acquisitions. Therefore, the scenario has not been uniformly irradiated by the radar signal, and sometimes the illumination time has been not enough for the proper SAR processing.

References

[Ref. 1] www.metasensing.com

[Ref. 2] https://snow.nasa.gov/snowex

[Ref. 3] Request for Proposal (TO RFP), Task 145, Ref: MIST – Subcontract, 27th July, 2016.

[Ref. 4] MS quote # MSQ_20160803_108, 3rd August 2016.

[Ref. 5] FFP contract Nr. MISTF-008 issued under prime contract Nr. NNG15CR64C "Mechanical Integrated Services and Technologies" (MIST), 6th December 2016.

[Ref. 6] SnowSAR for SnowEx Electrical ICD, MS-NAS-SNX-01-EIC-011, 9th November 2016.

[Ref. 7] https://www.novatel.com/assets/Documents/Papers/SPAN-CPT.pdf

[Ref. 8] https://www.novatel.com/assets/Documents/Waypoint/InertialExplorer.pdf

[Ref. 9] L.M.H. Ulander, H. Hellsten, and G. Stenstrm, "Synthetic-aperture radar processing using fast factorized back-projection," IEEE Trans. Aerosp. Electron. Syst., vol. 39, pp. 760–776, Jul. 2003.

[Ref. 10] A.W. Doerry, E.E. Bishop, J.A. Miller, "Basics of backprojections algorithm for processing SAR images", Sandia National Laboratories Albuquerque, New Mexico 87185 and Livermore, California 94550, Feb 2016.

[Ref. 11] http://srtm.csi.cgiar.org/SELECTION/inputCoord.asp

[Ref.12] A. Freeman, "Radiometric calibration of SAR image data". XVII Congress for Photogrammetry and Remote Sensing (ISPRS), 1992. [Online]. Available: http://bit.ly/1kbAujT

[Ref. 13] F. Sarti, "Remote sensing and SAR images processing characterization and speckle filtering in radar images", ESA radar remote sensing course, Tartu, Estonia, 16-20 April 2012.

[Ref. 14] A. L. Gray A, ,P.W. Vachon, et al. "Synthetic Aperture Radar Calibration Using Reference Reflectors", J. IEEE Trans on Geoscience and Remote Sensing. , Vol.: 28 Issue: 3, May 1990.

Appendix A – NetCDF data format

This Appendix provides information about the format and contents of the delivered NetCDF files.

File naming

An example of delivered file name of the SnowSAR NetCDF files is:

SAR_MLOOK_20170221202338_0_1_9.6G_VV_21_pres_16_fdc_415_498_581_665_748_831_914_997_1080.sar.rgo.sig.pow.db.nc

Where the fields are defined as follows:

SAR_MLOOK:	Multilooked SAR data
_20170221202338:	Starting date and time of the acquisition, in the YYYYMMDDHHMMSS format, where YYYY is the year, MM the month, DD the day, HH the hour, MM the minutes and SS the seconds, in UTC time.
_0	Frequency band: 0 and 1 are relative to X- and Ku- band, respectively.
_1	Multistatic: in case of a multistatic system this field identifies different nodes; SnowSAR is monostatic system, so all files are _1.
_9.6G	Operating frequency, G standing for Gigahertz.
_VV	Polarization channel, 1st letter is the transmitter, the 2nd is the receiver.
_21	Channel (in monostatic systems this field is redundant w.r.t. the polarization channel).
_pres_16	Presumming factor of 16
_Fdc_415_…._1080:	Doppler centroid frequencies which have been processed; this example is composed by 9 looks.

sar.rgo.sig.pow.db.nc Additional details of the applied processing: SAR data, geometrically calibrated, radiometrically calibrated, converted in power [dB], in netcdf format.

File dimensions

Each NetCDF file has 6 dimensions:

GroundRange = *10592*
CrossRange = *19648*
GPSTime = *20403*
AntPatternAngles = *361*
ModelTransformationTagRows = *4*
ModelTransformationTagCols = *4*

The *GroundRange* and *CrossRange* dimensions are related to the grid on top of which the focused SAR pixels are projected. This grid is uniformly sampled in space. The *GroundRange* and *CrossRange* dimensions refer to the number of samples the processed image has in ground-range and along-track directions, respectively.

The *GPStime* dimension gives the number of the equally spaced time samples of the post-processed navigation data.

The *AntPatternAngles* gives the number of samples describing the antenna patterns (both in azimuth and elevation), uniformly spaced between -180 to 180 degrees.

The *ModelTransformationTagRows and ModelTransformationTagCols* refer to the matrix (rows and columns) that relates the SAR image grid to the model space grid (geographical coordinates).

2D Variables

The SAR image is given as backscatter coefficient values:

SigmaImageAmplitude

Size: *10592x19648*

Dimensions: *GroundRange,CrossRange*

Datatype: *double*

Attributes:

long_name = 'sigma-naught calibrated and ground projected SAR image amplitude'

units = '[]'

The position of each pixel in the SAR image in WGS-84 ellipsoid is given by:

LatImage

Size: *5984x18512*

Dimensions: *GroundRange,CrossRange*

Datatype: *double*

Attributes:

long_name = 'latitude of the pixels in the image'

units = '[deg]'

LonImage

Size: *5984x18512*

Dimensions: *GroundRange,CrossRange*

Datatype: *double*

Attributes:

long_name = 'longitude of the pixels in the image'

units = '[deg]'

The *DEMImage* is the WGS-84 height model with the same geometry and same dimension of the processed SLC SAR data. It contains the WGS-84 height for each pixel of the SLC SAR data. The DEM heights are the ones used during SAR processing.

DEMImage

Size: 10592x19648

Dimensions: GroundRange,CrossRange

Datatype: single

Attributes:

long_name = 'Elevation (WGS84) of the pixels in the image'

units = '[m]'

CalImage gives the calibration factor used to radiometrically calibrate each pixel of the SAR image.

CalImage

Size: 10592x19648

Dimensions: GroundRange,CrossRange

Datatype: single

Attributes:

long_name = 'Calibration Factor for each pixel in the image'

units = '[dB]'

The position of antenna associated with each focused pixel is given explicitly through a matrix of the same size of the SAR image as follows:

OrbLatImage

Size: 5984x18512

Dimensions: GroundRange,CrossRange

Datatype: double

Attributes:

long_name = 'latitude of the sensor for each pixel in the image'

units = '[deg]'

OrbLonImage

Size: 5984x18512

Dimensions: GroundRange,CrossRange

Datatype: double

Attributes:

long_name = 'longtitude of the sensor for each pixel in the image'

units = '[deg]'

OrbHeightImage

Size: *5984x18512*

Dimensions: *GroundRange,CrossRange*

Datatype: *double*

Attributes:

long_name = 'Height above ellipsoid WGS84 of the sensor for each pixel in the image'

units = '[m]'

The *Orbitimage* is a LUT. It provides the index information that links the SAR geometry (2D) to a time tag relatively to the illumination instant after the focusing step.

OrbitImage

Size: *10592x19648*

Dimensions: GroundRange,CrossRange

Datatype: *single*

Attributes:

long_name = 'LUT to find the GPS time associated with the SLC image pixels'

units = '[]'

1D variables

The NetCDF file has the following 1D variables

The *GroundRange* variable defines the SAR image in ground range direction and dimension. The difference between two subsequent samples of the GroundRange variables give the ground-range spacing.

GroundRange

Size: *10592x1*

Dimensions: *GroundRange*

Datatype: *single*

Attributes:

long_name = 'Dimension of the image in ground range direction '

units = '[m]'

The *CrossRange* defines the SAR image in cross-range direction and dimension. The difference between two subsequent samples of the *CrossRange* variable give us the cross-range spacing.

CrossRange

Size: *19648x1*

Dimensions: *CrossRange*

Datatype: *single*

Attributes:

long_name = 'Dimension of the image along cross-range direction'

units = '[m]'

The *GPStime* variable gives the GPS time tag for each of the state vectors. The state vectors are the *OrbitLatitude*, *OrbitLongitude*, *OrbitHeight*, and rotations given by *OrbitHeading*, *OrbitRoll*, *OrbitPitch.* The above State vectors have the same dimension as *GPStime* and are associated with the SAR pixels through the *OrbitImage* LUT.

GPSTime

Size: *20403x1*

Dimensions: *GPSTime*

Datatype: *double*

Attributes:

long_name = 'GPS time (orbit)'

units = '[s]'

OrbitLatitude

Size: *20403x1*

Dimensions: *GPSTime*

Datatype: *double*

Attributes:

long_name = 'Latitude of the antenna orbit'

units = '[]'

OrbitLongitude

Size: *20403x1*

Dimensions: *GPSTime*

Datatype: *double*

Attributes:

long_name = 'Longitude of the antenna orbit'

units = '[]'

OrbitHeight

Size: *20403x1*

Dimensions: *GPSTime*

Datatype: *double*

Attributes:

long_name = 'Antenna height above WGS84'

units = '[deg.]'

OrbitHeading

Size: *20403x1*

Dimensions: *GPSTime*

Datatype: *double*

Attributes:

long_name = 'Heading (relative to the True North) angles'

units = '[deg.]'

OrbitRoll

Size: *20403x1*

Dimensions: *GPSTime*

Datatype: *double*

Attributes:

long_name = 'Roll angles'

units = '[deg.]'

OrbitPitch

Size: *20403x1*

Dimensions: *GPSTime*

Datatype: *double*

Attributes:

long_name = 'Pitch angles'

units = '[deg.]'

The *ModelTransformationTag* gives exact affine transformations between raster and model space (this Tag is the same one used in the geotiff file header)

ModelTransformationTag

Size: *4x4*

Dimensions: *ModelTransformationTagRows,ModelTransformationTagCols*

Datatype: *double*

Attributes:

long_name = 'ModelTransformationTag'

units = '[]'

The *AntPatternAngles* gives the angle at which the antenna gain has been measured. It varies from -180 to 180 degrees with a spacing of 1 deg.

AntPatternAngles

Size: *361x1*

Dimensions: *AntPatternAngles*

Datatype: *double*

Attributes:

long_name = 'Antenna pattern angular dependence'

units = '[deg.]'

The variables *TxElevationGain*, *TxAzimuthnGain*, *RxElevationGain* and *RxAzimuthGain* are the Elevation and Azimuth Gains of the transmitting and receiving antennas, respectively, at the corresponding antenna pattern angles.

TxElevationGain

Size: *361x1*

Dimensions: *AntPatternAngles*

Datatype: *double*

Attributes:

long_name = 'Transmitting Antenna elevation gain'

units = '[dB]'

TxAzimuthGain

Size: *361x1*

Dimensions: *AntPatternAngles*

Datatype: *double*

Attributes:

long_name = 'Transmitting Antenna azimuth gain'

units = '[dB]'

RxElevationGain

Size: *361x1*

Dimensions: *AntPatternAngles*

Datatype: *double*

Attributes:

long_name = 'Receiving Antenna elevation gain'

units = '[dB]'

RxAzimuthGain

Size: *361x1*

Dimensions: AntPatternAngles

Datatype: double

Attributes:

long_name = 'Receiving Antenna azimuth gain'

units = '[dB]'

Parameters

The following parameters gives the Year, Month, Day, and UTC hour, minutes and seconds for the first and last GPStime variable values.

StartYear

Size: 1x1

Dimensions:

Datatype: int32

Attributes:

long_name = 'Year of the Start of Acquisition'

units = '[year]'

StartMonth

Size: 1x1

Dimensions:

Datatype: int32

Attributes:

long_name = 'Month of the Start of Acquisition'

units = '[month]'

StartDay

Size: 1x1

Dimensions:

Datatype: int32

Attributes:

long_name = 'Day of the Start of Acquisition'

units = '[day]'

StartHour

Size: 1x1

Dimensions:

Datatype: int32

Attributes:

long_name = 'Hour of the Start of Acquisition'

units = '[hour]'

StartMin

Size: 1x1

Dimensions:

Datatype: int32

Attributes:

long_name = 'Minutes of the Start of Acquisition'

units = '[min]'

StartSec

Size: 1x1

Dimensions:

Datatype: single

Attributes:

long_name = 'Seconds of the Start of Acquisition'

units = '[sec]'

FinalYear

Size: 1x1

Dimensions:

Datatype: int32

Attributes:

long_name = 'Year of End of Acquisition'

units = '[year]'

FinalMonth

Size: 1x1

Dimensions:

Datatype: int32

Attributes:

long_name = 'Month of End of Acquisition'

units = '[month]'

FinalDay

Size: 1x1

Dimensions:

Datatype: int32

Attributes:

long_name = 'Day of End of Acquisition'

units = '[day]'

FinalHour

Size: *1x1*

Dimensions:

Datatype: *int32*

Attributes:

long_name = 'Hour of End of Acquisition'

units = '[hour]'

FinalMin

Size: *1x1*

Dimensions:

Datatype: *int32*

Attributes:

long_name = 'Minutes of End of Acquisition'

units = '[min]'

FinalSec

Size: *1x1*

Dimensions:

Datatype: *single*

Attributes:

long_name = 'Seconds of End of Acquisition'

units = '[sec]'

The *TxPolarization* and *RxPolarization* give the polarization of the transmitted and receiving antenna

TxPolarization

Size: *1x1*

Dimensions:

Datatype: *char*

Attributes:

long_name = 'TX Polarization'

units = '[]'

RxPolarization

Size: *1x1*

Dimensions:

Datatype: *char*

Attributes:

long_name = 'RX Polarization'

units = '[]'

LookDirection specifies which side (left or right) is the SAR system looking.

LookDirection

Size: 1x1

Dimensions:

Datatype: char

Attributes:

long_name = 'Look direction R = Right or L = Left'

units = '[]'

The following variables provide information about the pointing direction of the RF antennas.

TxPointEl

Size: 1x1

Dimensions:

Datatype: single

Attributes:

long_name = 'Tx antenna pointing in elevation '

units = '[deg.]'

TxPointAz

Size: 1x1

Dimensions:

Datatype: single

Attributes:

long_name = 'Tx antenna pointing in azimuth '

units = '[deg.]'

RxPointEl

Size: 1x1

Dimensions:

Datatype: single

Attributes:

long_name = 'Rx antenna pointing in elevation '

units = '[deg.]'

RxPointAz

Size: 1x1

Dimensions:

Datatype: *single*

Attributes:

long_name = 'Rx antenna pointing in azimuth '

units = '[deg.]'

The following parameters describes the operating radar frequency, transmitted bandwidth and operating PRF.

CentralFreq

Size: *1x1*

Dimensions:

Datatype: *single*

Attributes:

long_name = 'Central frequency'

units = '[Hz]'

TransmittedBandWidth

Size: *1x1*

Dimensions:

Datatype: *single*

Attributes:

long_name = 'Transmitted bandwidth'

units = '[Hz]'

PRF

Size: *1x1*

Dimensions:

Datatype: *single*

Attributes:

long_name = 'Pulse Repetition Frequency'

units = '[Hz]'

The average velocity of the aircraft during the acquisition is noted in the following variable:

MeanForwardVelocity

Size: *1x1*

Dimensions:

Datatype: *single*

Attributes:

long_name = 'Flight direction velocity'

units = '[m/s]'

During the processing the PRF is reduced by an integer factor given by the *DopplerPresumming* variable:

DopplerPresumming

Size: *1x1*

Dimensions:

Datatype: *single*

Attributes:

long_name = 'Doppler Presumming'

units = '[]'

During the SAR processing the range compressed data are filtered in the frequency domain according to the Doppler centroid and resolution.

The doppler centroid is computed as: $\frac{\text{MinProcessedDopper}+\text{MaxProcessedDoppler}}{2}$ where the *MinProcessedDoppler* and *MaxProcessedDoppler* give the frequency limits of the processed spectrum:

MinProcessedDoppler

Size: *1x1*

Dimensions:

Datatype: *single*

Attributes:

long_name = 'Minimum Processed Doppler'

units = '[Hz]'

MaxProcessedDoppler

Size: *1x1*

Dimensions:

Datatype: *single*

Attributes:

long_name = 'Maximum Processed Doppler'

units = '[Hz]'

The number of looks of the processed SAR image is given by the following variable:

Looks

Size: *1x1*

Dimensions:

Datatype: *int32*

Attributes:

long_name = 'Number of Looks (50% overlapping)'

units = '[]'

The geographical coordinates of the vertexes of the (rectangular) SAR image are given for reference:

Latitude11

Size: 1x1

Dimensions:

Datatype: double

Attributes:

long_name = 'Latitude of image corner (1, 1)'

units = '[deg.]'

Longitude11

Size: 1x1

Dimensions:

Datatype: double

Attributes:

long_name = 'Longitude of image corner (1, 1)'

units = '[deg.]'

Latitude12

Size: 1x1

Dimensions:

Datatype: double

Attributes:

long_name = 'Latitude of image corner (1, groundrange)'

units = '[deg.]'

Longitude12

Size: 1x1

Dimensions:

Datatype: double

Attributes:

long_name = 'Longitude of image corner (1, groundrange)'

units = '[deg.]'

Latitude21

Size: 1x1

Dimensions:

Datatype: double

Attributes:

long_name = 'Latitude of image corner (crossrange, 1)'

units = '[deg.]'

Longitude21

Size: 1x1

Dimensions:

Datatype: double

Attributes:

long_name = 'Longitude of image corner (crossrange, 1)'

units = '[deg.]'

Latitude22

Size: 1x1

Dimensions:

Datatype: double

Attributes:

long_name = 'Latitude of image corner (crossrange, groundrange)'

units = '[deg.]'

Longitude22

Size: 1x1

Dimensions:

Datatype: double

Attributes:

long_name = 'Longitude of image corner (crossrange, groundrange)'

units = '[deg.]'

The UTM zone of the grid is given as

UTMZone

Size: 1x1

Dimensions:

Datatype: int32

Attributes:

long_name = 'UTM zone'

units = '[]'

This field specifies if the measurements are performed in monostatic or bistatic configuration.

SystemType

Size: 1x1

Dimensions:

Datatype: *char*

Attributes:

long_name = 'System type: M for monostatitc, B for Bistatic'

units = '[]'

The SAR image pixels not corresponding to valid data are given as dummy values. This is set to -9999 as given by this parameter.

Dummy

Size: *1x1*

Dimensions:

Datatype: *int32*

Attributes:

long_name = 'Dummy value'

units = '[]'

Appendix B – Data inventory

The following tables list the delivered data tracks according to the date in which they have been acquired.

	Feb. 16th 2017 (X- and Ku-band)
1	SAR_MLOOK_20170216213331_0_1_9.6G_HH_12_pres_8_fdc_-293_-196_-98_0_97_195_292_390_488.sar.rgo.sig.pow.db.nc
2	SAR_MLOOK_20170216213331_0_1_9.6G_HV_11_pres_8_fdc_-293_-196_-98_0_97_195_292_390_488.sar.rgo.sig.pow.db.nc
3	SAR_MLOOK_20170216213331_0_1_9.6G_VH_22_pres_8_fdc_-293_-196_-98_0_97_195_292_390_488.sar.rgo.sig.pow.db.nc
4	SAR_MLOOK_20170216213331_0_1_9.6G_VV_21_pres_8_fdc_-293_-196_-98_0_97_195_292_390_488.sar.rgo.sig.pow.db.nc
5	SAR_MLOOK_20170216213331_1_1_17.2G_HH_12_pres_8_fdc_-293_-196_-98_0_97_195_292_390_488.sar.rgo.sig.pow.db.nc
6	SAR_MLOOK_20170216213331_1_1_17.2G_HV_11_pres_8_fdc_-293_-196_-98_0_97_195_292_390_488.sar.rgo.sig.pow.db.nc
7	SAR_MLOOK_20170216213331_1_1_17.2G_VH_22_pres_8_fdc_-293_-196_-98_0_97_195_292_390_488.sar.rgo.sig.pow.db.nc
8	SAR_MLOOK_20170216213331_1_1_17.2G_VV_21_pres_8_fdc_-293_-196_-98_0_97_195_292_390_488.sar.rgo.sig.pow.db.nc
9	SAR_MLOOK_20170216232346_0_1_9.6G_HH_12_pres_8_fdc_-293_-196_-98_0_97_195_292_390_488.sar.rgo.sig.pow.db.nc
10	SAR_MLOOK_20170216232346_0_1_9.6G_HV_11_pres_8_fdc_-293_-196_-98_0_97_195_292_390_488.sar.rgo.sig.pow.db.nc
11	SAR_MLOOK_20170216232346_0_1_9.6G_VH_22_pres_8_fdc_-293_-196_-98_0_97_195_292_390_488.sar.rgo.sig.pow.db.nc
12	SAR_MLOOK_20170216232346_0_1_9.6G_VV_21_pres_8_fdc_-293_-196_-98_0_97_195_292_390_488.sar.rgo.sig.pow.db.nc

	Feb. 18th 2017 (only X-band)
1	SAR_MLOOK_20170218163313_0_1_9.6G_HH_12_pres_8_fdc_292_390_488_585_683_781_878.sar.rgo.sig.pow.db.nc
2	SAR_MLOOK_20170218163313_0_1_9.6G_HV_11_pres_8_fdc_292_390_488_585_683_781_878.sar.rgo.sig.pow.db.nc
3	SAR_MLOOK_20170218163313_0_1_9.6G_VH_22_pres_8_fdc_292_390_488_585_683_781_878.sar.rgo.sig.pow.db.nc
4	SAR_MLOOK_20170218163313_0_1_9.6G_VV_21_pres_8_fdc_292_390_488_585_683_781_878.sar.rgo.sig.pow.db.nc
5	SAR_MLOOK_20170218164700_0_1_9.6G_HH_12_pres_8_fdc_292_390_488_585_683_781_878.sar.rgo.sig.pow.db.nc
6	SAR_MLOOK_20170218164700_0_1_9.6G_HV_11_pres_8_fdc_292_390_488_585_683_781_878.sar.rgo.sig.pow.db.nc
7	SAR_MLOOK_20170218164700_0_1_9.6G_VH_22_pres_8_fdc_292_390_488_585_683_781_878.sar.rgo.sig.pow.db.nc
8	SAR_MLOOK_20170218164700_0_1_9.6G_VV_21_pres_8_fdc_292_390_488_585_683_781_878.sar.rgo.sig.pow.db.nc
9	SAR_MLOOK_20170218170142_0_1_9.6G_HH_12_pres_8_fdc_585_683_781_878_976_1074_1171.sar.rgo.sig.pow.db.nc
10	SAR_MLOOK_20170218170142_0_1_9.6G_HV_11_pres_8_fdc_585_683_781_878_976_1074_1171.sar.rgo.sig.pow.db.nc
11	SAR_MLOOK_20170218170142_0_1_9.6G_VH_22_pres_8_fdc_585_683_781_878_976_1074_1171.sar.rgo.sig.pow.db.nc
12	SAR_MLOOK_20170218170142_0_1_9.6G_VV_21_pres_8_fdc_585_683_781_878_976_1074_1171.sar.rgo.sig.pow.db.nc
13	SAR_MLOOK_20170218173226_0_1_9.6G_HH_12_pres_8_fdc_166_332_498_665.sar.rgo.sig.pow.db.nc
14	SAR_MLOOK_20170218173226_0_1_9.6G_HV_11_pres_8_fdc_166_332_498_665.sar.rgo.sig.pow.db.nc
15	SAR_MLOOK_20170218173226_0_1_9.6G_VH_22_pres_8_fdc_166_332_498_665.sar.rgo.sig.pow.db.nc
16	SAR_MLOOK_20170218173226_0_1_9.6G_VV_21_pres_8_fdc_166_332_498_665.sar.rgo.sig.pow.db.nc
17	SAR_MLOOK_20170218173445_0_1_9.6G_HH_12_pres_16_fdc_113_227_341_455.sar.rgo.sig.pow.db.nc
18	SAR_MLOOK_20170218173445_0_1_9.6G_HV_11_pres_16_fdc_113_227_341_455.sar.rgo.sig.pow.db.nc
19	SAR_MLOOK_20170218173445_0_1_9.6G_VH_22_pres_16_fdc_113_227_341_455.sar.rgo.sig.pow.db.nc
20	SAR_MLOOK_20170218173445_0_1_9.6G_VV_21_pres_16_fdc_113_227_341_455.sar.rgo.sig.pow.db.nc
21	SAR_MLOOK_20170218174831_0_1_9.6G_HH_12_pres_16_fdc_249_332_415_498_581.sar.rgo.sig.pow.db.nc
22	SAR_MLOOK_20170218174831_0_1_9.6G_HV_11_pres_16_fdc_249_332_415_498_581.sar.rgo.sig.pow.db.nc
23	SAR_MLOOK_20170218174831_0_1_9.6G_VH_22_pres_16_fdc_249_332_415_498_581.sar.rgo.sig.pow.db.nc
24	SAR_MLOOK_20170218174831_0_1_9.6G_VV_21_pres_16_fdc_249_332_415_498_581.sar.rgo.sig.pow.db.nc
25	SAR_MLOOK_20170218174933_0_1_9.6G_HH_12_pres_16_fdc_227_341_455_569.sar.rgo.sig.pow.db.nc
26	SAR_MLOOK_20170218174933_0_1_9.6G_HV_11_pres_16_fdc_227_341_455_569.sar.rgo.sig.pow.db.nc

27	SAR_MLOOK_20170218174933_0_1_9.6G_VH_22_pres_16_fdc_227_341_455_569.sar.rgo.sig.pow.db.nc
28	SAR_MLOOK_20170218174933_0_1_9.6G_VV_21_pres_16_fdc_227_341_455_569.sar.rgo.sig.pow.db.nc
29	SAR_MLOOK_20170218175045_0_1_9.6G_HH_12_pres_16_fdc_113_227_341_455.sar.rgo.sig.pow.db.nc
30	SAR_MLOOK_20170218175045_0_1_9.6G_HV_11_pres_16_fdc_113_227_341_455.sar.rgo.sig.pow.db.nc
31	SAR_MLOOK_20170218175045_0_1_9.6G_VH_22_pres_16_fdc_113_227_341_455.sar.rgo.sig.pow.db.nc
32	SAR_MLOOK_20170218175045_0_1_9.6G_VV_21_pres_16_fdc_113_227_341_455.sar.rgo.sig.pow.db.nc

	Feb. 21st 2017 (X-band)
1	SAR_MLOOK_20170221172126_0_1_9.6G_HH_12_pres_16_fdc_415_498_581_665_748_831_914_997_1080.sar.rgo.sig.pow.db.nc
2	SAR_MLOOK_20170221172126_0_1_9.6G_HV_11_pres_16_fdc_415_498_581_665_748_831_914_997_1080.sar.rgo.sig.pow.db.nc
3	SAR_MLOOK_20170221172126_0_1_9.6G_VH_22_pres_16_fdc_415_498_581_665_748_831_914_997_1080.sar.rgo.sig.pow.db.nc
4	SAR_MLOOK_20170221172126_0_1_9.6G_VV_21_pres_16_fdc_415_498_581_665_748_831_914_997_1080.sar.rgo.sig.pow.db.nc
5	SAR_MLOOK_20170221173206_0_1_9.6G_HH_12_pres_16_fdc_415_498_581_665_748_831_914_997_1080.sar.rgo.sig.pow.db.nc
6	SAR_MLOOK_20170221173206_0_1_9.6G_HV_11_pres_16_fdc_415_498_581_665_748_831_914_997_1080.sar.rgo.sig.pow.db.nc
7	SAR_MLOOK_20170221173206_0_1_9.6G_VH_22_pres_16_fdc_415_498_581_665_748_831_914_997_1080.sar.rgo.sig.pow.db.nc
8	SAR_MLOOK_20170221173206_0_1_9.6G_VV_21_pres_16_fdc_415_498_581_665_748_831_914_997_1080.sar.rgo.sig.pow.db.nc
9	SAR_MLOOK_20170221174335_0_1_9.6G_HH_12_pres_16_fdc_-167_-84_0_83_166_249_332_415_498.sar.rgo.sig.pow.db.nc
10	SAR_MLOOK_20170221174335_0_1_9.6G_HV_11_pres_16_fdc_-167_-84_0_83_166_249_332_415_498.sar.rgo.sig.pow.db.nc
11	SAR_MLOOK_20170221174335_0_1_9.6G_VH_22_pres_16_fdc_-167_-84_0_83_166_249_332_415_498.sar.rgo.sig.pow.db.nc
12	SAR_MLOOK_20170221174335_0_1_9.6G_VV_21_pres_16_fdc_-167_-84_0_83_166_249_332_415_498.sar.rgo.sig.pow.db.nc
13	SAR_MLOOK_20170221175530_0_1_9.6G_HH_12_pres_16_fdc_-333_-250_-167_-84_0_83_166_249_332.sar.rgo.sig.pow.db.nc
14	SAR_MLOOK_20170221175530_0_1_9.6G_HV_11_pres_16_fdc_-333_-250_-167_-84_0_83_166_249_332.sar.rgo.sig.pow.db.nc
15	SAR_MLOOK_20170221175530_0_1_9.6G_VH_22_pres_16_fdc_-333_-250_-167_-84_0_83_166_249_332.sar.rgo.sig.pow.db.nc
16	SAR_MLOOK_20170221175530_0_1_9.6G_VV_21_pres_16_fdc_-333_-250_-167_-84_0_83_166_249_332.sar.rgo.sig.pow.db.nc
17	SAR_MLOOK_20170221180329_0_1_9.6G_HH_12_pres_16_fdc_166_249_332_415_498_581_665_748_831.sar.rgo.sig.pow.db.nc
18	SAR_MLOOK_20170221180329_0_1_9.6G_HV_11_pres_16_fdc_166_249_332_415_498_581_665_748_831.sar.rgo.sig.pow.db.nc
19	SAR_MLOOK_20170221180329_0_1_9.6G_VH_22_pres_16_fdc_166_249_332_415_498_581_665_748_831.sar.rgo.sig.pow.db.nc
20	SAR_MLOOK_20170221180329_0_1_9.6G_VV_21_pres_16_fdc_166_249_332_415_498_581_665_748_831.sar.rgo.sig.pow.db.nc
21	SAR_MLOOK_20170221181138_0_1_9.6G_HH_12_pres_16_fdc_-333_-250_-167_-84_0_83_166_249_332.sar.rgo.sig.pow.db.nc
22	SAR_MLOOK_20170221181138_0_1_9.6G_HV_11_pres_16_fdc_-333_-250_-167_-84_0_83_166_249_332.sar.rgo.sig.pow.db.nc
23	SAR_MLOOK_20170221181138_0_1_9.6G_VH_22_pres_16_fdc_-333_-250_-167_-84_0_83_166_249_332.sar.rgo.sig.pow.db.nc
24	SAR_MLOOK_20170221181138_0_1_9.6G_VV_21_pres_16_fdc_-333_-250_-167_-84_0_83_166_249_332.sar.rgo.sig.pow.db.nc
25	SAR_MLOOK_20170221181936_0_1_9.6G_HH_12_pres_16_fdc_83_166_249_332_415_498_581_665_748.sar.rgo.sig.pow.db.nc
26	SAR_MLOOK_20170221181936_0_1_9.6G_HV_11_pres_16_fdc_83_166_249_332_415_498_581_665_748.sar.rgo.sig.pow.db.nc

27	SAR_MLOOK_20170221181936_0_1_9.6G_VH_22_pres_16_fdc_83_166_249_332_415_498_581_665_748.sar.rgo.sig.pow.db.nc
28	SAR_MLOOK_20170221181936_0_1_9.6G_VV_21_pres_16_fdc_83_166_249_332_415_498_581_665_748.sar.rgo.sig.pow.db.nc
29	SAR_MLOOK_20170221182722_0_1_9.6G_HH_12_pres_16_fdc_-333_-250_-167_-84_0_83_166_249_332.sar.rgo.sig.pow.db.nc
30	SAR_MLOOK_20170221182722_0_1_9.6G_HV_11_pres_16_fdc_-333_-250_-167_-84_0_83_166_249_332.sar.rgo.sig.pow.db.nc
31	SAR_MLOOK_20170221182722_0_1_9.6G_VH_22_pres_16_fdc_-333_-250_-167_-84_0_83_166_249_332.sar.rgo.sig.pow.db.nc
32	SAR_MLOOK_20170221182722_0_1_9.6G_VV_21_pres_16_fdc_-333_-250_-167_-84_0_83_166_249_332.sar.rgo.sig.pow.db.nc
33	SAR_MLOOK_20170221183532_0_1_9.6G_HH_12_pres_16_fdc_83_166_249_332_415_498_581_665_748.sar.rgo.sig.pow.db.nc
34	SAR_MLOOK_20170221183532_0_1_9.6G_HV_11_pres_16_fdc_83_166_249_332_415_498_581_665_748.sar.rgo.sig.pow.db.nc
35	SAR_MLOOK_20170221183532_0_1_9.6G_VH_22_pres_16_fdc_83_166_249_332_415_498_581_665_748.sar.rgo.sig.pow.db.nc
36	SAR_MLOOK_20170221183532_0_1_9.6G_VV_21_pres_16_fdc_83_166_249_332_415_498_581_665_748.sar.rgo.sig.pow.db.nc
37	SAR_MLOOK_20170221184320_0_1_9.6G_HH_12_pres_16_fdc_-333_-250_-167_-84_0_83_166_249_332.sar.rgo.sig.pow.db.nc
38	SAR_MLOOK_20170221184320_0_1_9.6G_HV_11_pres_16_fdc_-333_-250_-167_-84_0_83_166_249_332.sar.rgo.sig.pow.db.nc
39	SAR_MLOOK_20170221184320_0_1_9.6G_VH_22_pres_16_fdc_-333_-250_-167_-84_0_83_166_249_332.sar.rgo.sig.pow.db.nc
40	SAR_MLOOK_20170221184320_0_1_9.6G_VV_21_pres_16_fdc_-333_-250_-167_-84_0_83_166_249_332.sar.rgo.sig.pow.db.nc
41	SAR_MLOOK_20170221185115_0_1_9.6G_HH_12_pres_16_fdc_249_332_415_498_581_665_748_831_914.sar.rgo.sig.pow.db.nc
42	SAR_MLOOK_20170221185115_0_1_9.6G_HV_11_pres_16_fdc_249_332_415_498_581_665_748_831_914.sar.rgo.sig.pow.db.nc
43	SAR_MLOOK_20170221185115_0_1_9.6G_VH_22_pres_16_fdc_249_332_415_498_581_665_748_831_914.sar.rgo.sig.pow.db.nc
44	SAR_MLOOK_20170221185115_0_1_9.6G_VV_21_pres_16_fdc_249_332_415_498_581_665_748_831_914.sar.rgo.sig.pow.db.nc
45	SAR_MLOOK_20170221185902_0_1_9.6G_HH_12_pres_16_fdc_-333_-250_-167_-84_0_83_166_249_332.sar.rgo.sig.pow.db.nc
46	SAR_MLOOK_20170221185902_0_1_9.6G_HV_11_pres_16_fdc_-333_-250_-167_-84_0_83_166_249_332.sar.rgo.sig.pow.db.nc
47	SAR_MLOOK_20170221185902_0_1_9.6G_VH_22_pres_16_fdc_-333_-250_-167_-84_0_83_166_249_332.sar.rgo.sig.pow.db.nc
48	SAR_MLOOK_20170221185902_0_1_9.6G_VV_21_pres_16_fdc_-333_-250_-167_-84_0_83_166_249_332.sar.rgo.sig.pow.db.nc
49	SAR_MLOOK_20170221190734_0_1_9.6G_HH_12_pres_16_fdc_83_166_249_332_415_498_581_665_748.sar.rgo.sig.pow.db.nc
50	SAR_MLOOK_20170221190734_0_1_9.6G_HV_11_pres_16_fdc_83_166_249_332_415_498_581_665_748.sar.rgo.sig.pow.db.nc
51	SAR_MLOOK_20170221190734_0_1_9.6G_VH_22_pres_16_fdc_83_166_249_332_415_498_581_665_748.sar.rgo.sig.pow.db.nc
52	SAR_MLOOK_20170221190734_0_1_9.6G_VV_21_pres_16_fdc_83_166_249_332_415_498_581_665_748.sar.rgo.sig.pow.db.nc
53	SAR_MLOOK_20170221191537_0_1_9.6G_HH_12_pres_16_fdc_-250_-167_-84_0_83_166_249_332_415.sar.rgo.sig.pow.db.nc

54	SAR_MLOOK_20170221191537_0_1_9.6G_HV_11_pres_16_fdc_-250_-167_-84_0_83_166_249_332_415.sar.rgo.sig.pow.db.nc
55	SAR_MLOOK_20170221191537_0_1_9.6G_VH_22_pres_16_fdc_-250_-167_-84_0_83_166_249_332_415.sar.rgo.sig.pow.db.nc
56	SAR_MLOOK_20170221191537_0_1_9.6G_VV_21_pres_16_fdc_-250_-167_-84_0_83_166_249_332_415.sar.rgo.sig.pow.db.nc
57	SAR_MLOOK_20170221192430_0_1_9.6G_HH_12_pres_16_fdc_166_249_332_415_498_581_665_748_831.sar.rgo.sig.pow.db.nc
58	SAR_MLOOK_20170221192430_0_1_9.6G_HV_11_pres_16_fdc_166_249_332_415_498_581_665_748_831.sar.rgo.sig.pow.db.nc
59	SAR_MLOOK_20170221192430_0_1_9.6G_VH_22_pres_16_fdc_166_249_332_415_498_581_665_748_831.sar.rgo.sig.pow.db.nc
60	SAR_MLOOK_20170221192430_0_1_9.6G_VV_21_pres_16_fdc_166_249_332_415_498_581_665_748_831.sar.rgo.sig.pow.db.nc
61	SAR_MLOOK_20170221193219_0_1_9.6G_HH_12_pres_16_fdc_-250_-167_-84_0_83_166_249_332_415.sar.rgo.sig.pow.db.nc
62	SAR_MLOOK_20170221193219_0_1_9.6G_HV_11_pres_16_fdc_-250_-167_-84_0_83_166_249_332_415.sar.rgo.sig.pow.db.nc
63	SAR_MLOOK_20170221193219_0_1_9.6G_VH_22_pres_16_fdc_-250_-167_-84_0_83_166_249_332_415.sar.rgo.sig.pow.db.nc
64	SAR_MLOOK_20170221193219_0_1_9.6G_VV_21_pres_16_fdc_-250_-167_-84_0_83_166_249_332_415.sar.rgo.sig.pow.db.nc
65	SAR_MLOOK_20170221194214_0_1_9.6G_HH_12_pres_16_fdc_-84_0_83_166_249_332_415_498_581.sar.rgo.sig.pow.db.nc
66	SAR_MLOOK_20170221194214_0_1_9.6G_HV_11_pres_16_fdc_-84_0_83_166_249_332_415_498_581.sar.rgo.sig.pow.db.nc
67	SAR_MLOOK_20170221194214_0_1_9.6G_VH_22_pres_16_fdc_-84_0_83_166_249_332_415_498_581.sar.rgo.sig.pow.db.nc
68	SAR_MLOOK_20170221194214_0_1_9.6G_VV_21_pres_16_fdc_-84_0_83_166_249_332_415_498_581.sar.rgo.sig.pow.db.nc
69	SAR_MLOOK_20170221195116_0_1_9.6G_HH_12_pres_16_fdc_-250_-167_-84_0_83_166_249_332_415.sar.rgo.sig.pow.db.nc
70	SAR_MLOOK_20170221195116_0_1_9.6G_HV_11_pres_16_fdc_-250_-167_-84_0_83_166_249_332_415.sar.rgo.sig.pow.db.nc
71	SAR_MLOOK_20170221195116_0_1_9.6G_VH_22_pres_16_fdc_-250_-167_-84_0_83_166_249_332_415.sar.rgo.sig.pow.db.nc
72	SAR_MLOOK_20170221195116_0_1_9.6G_VV_21_pres_16_fdc_-250_-167_-84_0_83_166_249_332_415.sar.rgo.sig.pow.db.nc
73	SAR_MLOOK_20170221200014_0_1_9.6G_HH_12_pres_16_fdc_-84_0_83_166_249_332_415_498_581.sar.rgo.sig.pow.db.nc
74	SAR_MLOOK_20170221200014_0_1_9.6G_HV_11_pres_16_fdc_-84_0_83_166_249_332_415_498_581.sar.rgo.sig.pow.db.nc
75	SAR_MLOOK_20170221200014_0_1_9.6G_VH_22_pres_16_fdc_-84_0_83_166_249_332_415_498_581.sar.rgo.sig.pow.db.nc
76	SAR_MLOOK_20170221200014_0_1_9.6G_VV_21_pres_16_fdc_-84_0_83_166_249_332_415_498_581.sar.rgo.sig.pow.db.nc
77	SAR_MLOOK_20170221201129_0_1_9.6G_HH_12_pres_16_fdc_249_332_415_498_581_665_748_831_914.sar.rgo.sig.pow.db.nc
78	SAR_MLOOK_20170221201129_0_1_9.6G_HV_11_pres_16_fdc_249_332_415_498_581_665_748_831_914.sar.rgo.sig.pow.db.nc
79	SAR_MLOOK_20170221201129_0_1_9.6G_VH_22_pres_16_fdc_249_332_415_498_581_665_748_831_914.sar.rgo.sig.pow.db.nc
80	SAR_MLOOK_20170221201129_0_1_9.6G_VV_21_pres_16_fdc_249_332_415_498_581_665_748_831_914.sar.rgo.sig.pow.db.nc

81	SAR_MLOOK_20170221202338_0_1_9.6G_HH_12_pres_16_fdc_415_498_581_665_748_831_914_997_1080.sar.rgo.sig.pow.db.nc
82	SAR_MLOOK_20170221202338_0_1_9.6G_HV_11_pres_16_fdc_415_498_581_665_748_831_914_997_1080.sar.rgo.sig.pow.db.nc
83	SAR_MLOOK_20170221202338_0_1_9.6G_VH_22_pres_16_fdc_415_498_581_665_748_831_914_997_1080.sar.rgo.sig.pow.db.nc
84	SAR_MLOOK_20170221202338_0_1_9.6G_VV_21_pres_16_fdc_415_498_581_665_748_831_914_997_1080.sar.rgo.sig.pow.db.nc
	Feb. 21st 2017 (Ku-band)
1	SAR_MLOOK_20170221172126_1_1_17.2G_HH_12_pres_16_fdc_831_914_997_1080_1163_1246_1330_1413_1496.sar.rgo.sig.pow.db.nc
2	SAR_MLOOK_20170221172126_1_1_17.2G_HV_11_pres_16_fdc_831_914_997_1080_1163_1246_1330_1413_1496.sar.rgo.sig.pow.db.nc
3	SAR_MLOOK_20170221172126_1_1_17.2G_VH_22_pres_16_fdc_831_914_997_1080_1163_1246_1330_1413_1496.sar.rgo.sig.pow.db.nc
4	SAR_MLOOK_20170221172126_1_1_17.2G_VV_21_pres_16_fdc_831_914_997_1080_1163_1246_1330_1413_1496.sar.rgo.sig.pow.db.nc
5	SAR_MLOOK_20170221173206_1_1_17.2G_HH_12_pres_16_fdc_831_914_997_1080_1163_1246_1330_1413_1496.sar.rgo.sig.pow.db.nc
6	SAR_MLOOK_20170221173206_1_1_17.2G_HV_11_pres_16_fdc_831_914_997_1080_1163_1246_1330_1413_1496.sar.rgo.sig.pow.db.nc
7	SAR_MLOOK_20170221173206_1_1_17.2G_VH_22_pres_16_fdc_831_914_997_1080_1163_1246_1330_1413_1496.sar.rgo.sig.pow.db.nc
8	SAR_MLOOK_20170221173206_1_1_17.2G_VV_21_pres_16_fdc_831_914_997_1080_1163_1246_1330_1413_1496.sar.rgo.sig.pow.db.nc
9	SAR_MLOOK_20170221174335_1_1_17.2G_HH_12_pres_16_fdc_0_83_166_249_332_415_498_581_665.sar.rgo.sig.pow.db.nc
10	SAR_MLOOK_20170221174335_1_1_17.2G_HV_11_pres_16_fdc_0_83_166_249_332_415_498_581_665.sar.rgo.sig.pow.db.nc
11	SAR_MLOOK_20170221174335_1_1_17.2G_VH_22_pres_16_fdc_0_83_166_249_332_415_498_581_665.sar.rgo.sig.pow.db.nc
12	SAR_MLOOK_20170221174335_1_1_17.2G_VV_21_pres_16_fdc_0_83_166_249_332_415_498_581_665.sar.rgo.sig.pow.db.nc
13	SAR_MLOOK_20170221175530_1_1_17.2G_HH_12_pres_16_fdc_-333_-250_-167_-84_0_83_166_249_332.sar.rgo.sig.pow.db.nc
14	SAR_MLOOK_20170221175530_1_1_17.2G_HV_11_pres_16_fdc_-333_-250_-167_-84_0_83_166_249_332.sar.rgo.sig.pow.db.nc
15	SAR_MLOOK_20170221175530_1_1_17.2G_VH_22_pres_16_fdc_-333_-250_-167_-84_0_83_166_249_332.sar.rgo.sig.pow.db.nc
16	SAR_MLOOK_20170221175530_1_1_17.2G_VV_21_pres_16_fdc_-333_-250_-167_-84_0_83_166_249_332.sar.rgo.sig.pow.db.nc
17	SAR_MLOOK_20170221180329_1_1_17.2G_HH_12_pres_16_fdc_498_581_665_748_831_914_997_1080_1163.sar.rgo.sig.pow.db.nc
18	SAR_MLOOK_20170221180329_1_1_17.2G_HV_11_pres_16_fdc_498_581_665_748_831_914_997_1080_1163.sar.rgo.sig.pow.db.nc
19	SAR_MLOOK_20170221180329_1_1_17.2G_VH_22_pres_16_fdc_498_581_665_748_831_914_997_1080_1163.sar.rgo.sig.pow.db.nc
20	SAR_MLOOK_20170221180329_1_1_17.2G_VV_21_pres_16_fdc_498_581_665_748_831_914_997_1080_1163.sar.rgo.sig.pow.db.nc
21	SAR_MLOOK_20170221181138_1_1_17.2G_HH_12_pres_16_fdc_-333_-250_-167_-84_0_83_166_249_332.sar.rgo.sig.pow.db.nc
22	SAR_MLOOK_20170221181138_1_1_17.2G_HV_11_pres_16_fdc_-333_-250_-167_-84_0_83_166_249_332.sar.rgo.sig.pow.db.nc
23	SAR_MLOOK_20170221181138_1_1_17.2G_VH_22_pres_16_fdc_-333_-250_-167_-84_0_83_166_249_332.sar.rgo.sig.pow.db.nc

24	SAR_MLOOK_20170221181138_1_1_17.2G_VV_21_pres_16_fdc_-333_-250_-167_-84_0_83_166_249_332.sar.rgo.sig.pow.db.nc
25	SAR_MLOOK_20170221181936_1_1_17.2G_HH_12_pres_16_fdc_332_415_498_581_665_748_831_914_997.sar.rgo.sig.pow.db.nc
26	SAR_MLOOK_20170221181936_1_1_17.2G_HV_11_pres_16_fdc_332_415_498_581_665_748_831_914_997.sar.rgo.sig.pow.db.nc
27	SAR_MLOOK_20170221181936_1_1_17.2G_VH_22_pres_16_fdc_332_415_498_581_665_748_831_914_997.sar.rgo.sig.pow.db.nc
28	SAR_MLOOK_20170221181936_1_1_17.2G_VV_21_pres_16_fdc_332_415_498_581_665_748_831_914_997.sar.rgo.sig.pow.db.nc
29	SAR_MLOOK_20170221182722_1_1_17.2G_HH_12_pres_16_fdc_-333_-250_-167_-84_0_83_166_249_332.sar.rgo.sig.pow.db.nc
30	SAR_MLOOK_20170221182722_1_1_17.2G_HV_11_pres_16_fdc_-333_-250_-167_-84_0_83_166_249_332.sar.rgo.sig.pow.db.nc
31	SAR_MLOOK_20170221182722_1_1_17.2G_VH_22_pres_16_fdc_-333_-250_-167_-84_0_83_166_249_332.sar.rgo.sig.pow.db.nc
32	SAR_MLOOK_20170221182722_1_1_17.2G_VV_21_pres_16_fdc_-333_-250_-167_-84_0_83_166_249_332.sar.rgo.sig.pow.db.nc
33	SAR_MLOOK_20170221183532_1_1_17.2G_HH_12_pres_16_fdc_332_415_498_581_665_748_831_914_997.sar.rgo.sig.pow.db.nc
34	SAR_MLOOK_20170221183532_1_1_17.2G_HV_11_pres_16_fdc_332_415_498_581_665_748_831_914_997.sar.rgo.sig.pow.db.nc
35	SAR_MLOOK_20170221183532_1_1_17.2G_VH_22_pres_16_fdc_332_415_498_581_665_748_831_914_997.sar.rgo.sig.pow.db.nc
36	SAR_MLOOK_20170221183532_1_1_17.2G_VV_21_pres_16_fdc_332_415_498_581_665_748_831_914_997.sar.rgo.sig.pow.db.nc
37	SAR_MLOOK_20170221184320_1_1_17.2G_HH_12_pres_16_fdc_-333_-250_-167_-84_0_83_166_249_332.sar.rgo.sig.pow.db.nc
38	SAR_MLOOK_20170221184320_1_1_17.2G_HV_11_pres_16_fdc_-333_-250_-167_-84_0_83_166_249_332.sar.rgo.sig.pow.db.nc
39	SAR_MLOOK_20170221184320_1_1_17.2G_VH_22_pres_16_fdc_-333_-250_-167_-84_0_83_166_249_332.sar.rgo.sig.pow.db.nc
40	SAR_MLOOK_20170221184320_1_1_17.2G_VV_21_pres_16_fdc_-333_-250_-167_-84_0_83_166_249_332.sar.rgo.sig.pow.db.nc
41	SAR_MLOOK_20170221185115_1_1_17.2G_HH_12_pres_16_fdc_581_665_748_831_914_997_1080_1163_1246.sar.rgo.sig.pow.db.nc
42	SAR_MLOOK_20170221185115_1_1_17.2G_HV_11_pres_16_fdc_581_665_748_831_914_997_1080_1163_1246.sar.rgo.sig.pow.db.nc
43	SAR_MLOOK_20170221185115_1_1_17.2G_VH_22_pres_16_fdc_581_665_748_831_914_997_1080_1163_1246.sar.rgo.sig.pow.db.nc
44	SAR_MLOOK_20170221185115_1_1_17.2G_VV_21_pres_16_fdc_581_665_748_831_914_997_1080_1163_1246.sar.rgo.sig.pow.db.nc
45	SAR_MLOOK_20170221185902_1_1_17.2G_HH_12_pres_16_fdc_-333_-250_-167_-84_0_83_166_249_332.sar.rgo.sig.pow.db.nc
46	SAR_MLOOK_20170221185902_1_1_17.2G_HV_11_pres_16_fdc_-333_-250_-167_-84_0_83_166_249_332.sar.rgo.sig.pow.db.nc
47	SAR_MLOOK_20170221185902_1_1_17.2G_VH_22_pres_16_fdc_-333_-250_-167_-84_0_83_166_249_332.sar.rgo.sig.pow.db.nc
48	SAR_MLOOK_20170221185902_1_1_17.2G_VV_21_pres_16_fdc_-333_-250_-167_-84_0_83_166_249_332.sar.rgo.sig.pow.db.nc
49	SAR_MLOOK_20170221190734_1_1_17.2G_HH_12_pres_16_fdc_332_415_498_581_665_748_831_914_997.sar.rgo.sig.pow.db.nc
50	SAR_MLOOK_20170221190734_1_1_17.2G_HV_11_pres_16_fdc_332_415_498_581_665_748_831_914_997.sar.rgo.sig.pow.db.nc

51	SAR_MLOOK_20170221190734_1_1_17.2G_VH_22_pres_16_fdc_332_415_498_581_665_748_831_914_997.sar.rgo.sig.pow.db.nc
52	SAR_MLOOK_20170221190734_1_1_17.2G_VV_21_pres_16_fdc_332_415_498_581_665_748_831_914_997.sar.rgo.sig.pow.db.nc
53	SAR_MLOOK_20170221191537_1_1_17.2G_HH_12_pres_16_fdc_-250_-167_-84_0_83_166_249_332_415.sar.rgo.sig.pow.db.nc
54	SAR_MLOOK_20170221191537_1_1_17.2G_HV_11_pres_16_fdc_-250_-167_-84_0_83_166_249_332_415.sar.rgo.sig.pow.db.nc
55	SAR_MLOOK_20170221191537_1_1_17.2G_VH_22_pres_16_fdc_-250_-167_-84_0_83_166_249_332_415.sar.rgo.sig.pow.db.nc
56	SAR_MLOOK_20170221191537_1_1_17.2G_VV_21_pres_16_fdc_-250_-167_-84_0_83_166_249_332_415.sar.rgo.sig.pow.db.nc
57	SAR_MLOOK_20170221192430_1_1_17.2G_HH_12_pres_16_fdc_498_581_665_748_831_914_997_1080_1163.sar.rgo.sig.pow.db.nc
58	SAR_MLOOK_20170221192430_1_1_17.2G_HV_11_pres_16_fdc_498_581_665_748_831_914_997_1080_1163.sar.rgo.sig.pow.db.nc
59	SAR_MLOOK_20170221192430_1_1_17.2G_VH_22_pres_16_fdc_498_581_665_748_831_914_997_1080_1163.sar.rgo.sig.pow.db.nc
60	SAR_MLOOK_20170221192430_1_1_17.2G_VV_21_pres_16_fdc_498_581_665_748_831_914_997_1080_1163.sar.rgo.sig.pow.db.nc
61	SAR_MLOOK_20170221193219_1_1_17.2G_HH_12_pres_16_fdc_-250_-167_-84_0_83_166_249_332_415.sar.rgo.sig.pow.db.nc
62	SAR_MLOOK_20170221193219_1_1_17.2G_HV_11_pres_16_fdc_-250_-167_-84_0_83_166_249_332_415.sar.rgo.sig.pow.db.nc
63	SAR_MLOOK_20170221193219_1_1_17.2G_VH_22_pres_16_fdc_-250_-167_-84_0_83_166_249_332_415.sar.rgo.sig.pow.db.nc
64	SAR_MLOOK_20170221193219_1_1_17.2G_VV_21_pres_16_fdc_-250_-167_-84_0_83_166_249_332_415.sar.rgo.sig.pow.db.nc
65	SAR_MLOOK_20170221194214_1_1_17.2G_HH_12_pres_16_fdc_83_166_249_332_415_498_581_665_748.sar.rgo.sig.pow.db.nc
66	SAR_MLOOK_20170221194214_1_1_17.2G_HV_11_pres_16_fdc_83_166_249_332_415_498_581_665_748.sar.rgo.sig.pow.db.nc
67	SAR_MLOOK_20170221194214_1_1_17.2G_VH_22_pres_16_fdc_83_166_249_332_415_498_581_665_748.sar.rgo.sig.pow.db.nc
68	SAR_MLOOK_20170221194214_1_1_17.2G_VV_21_pres_16_fdc_83_166_249_332_415_498_581_665_748.sar.rgo.sig.pow.db.nc
69	SAR_MLOOK_20170221195116_1_1_17.2G_HH_12_pres_16_fdc_-167_-84_0_83_166_249_332_415_498.sar.rgo.sig.pow.db.nc
70	SAR_MLOOK_20170221195116_1_1_17.2G_HV_11_pres_16_fdc_-167_-84_0_83_166_249_332_415_498.sar.rgo.sig.pow.db.nc
71	SAR_MLOOK_20170221195116_1_1_17.2G_VH_22_pres_16_fdc_-167_-84_0_83_166_249_332_415_498.sar.rgo.sig.pow.db.nc
72	SAR_MLOOK_20170221195116_1_1_17.2G_VV_21_pres_16_fdc_-167_-84_0_83_166_249_332_415_498.sar.rgo.sig.pow.db.nc
73	SAR_MLOOK_20170221200014_1_1_17.2G_HH_12_pres_16_fdc_166_249_332_415_498_581_665_748_831.sar.rgo.sig.pow.db.nc
74	SAR_MLOOK_20170221200014_1_1_17.2G_HV_11_pres_16_fdc_166_249_332_415_498_581_665_748_831.sar.rgo.sig.pow.db.nc
75	SAR_MLOOK_20170221200014_1_1_17.2G_VH_22_pres_16_fdc_166_249_332_415_498_581_665_748_831.sar.rgo.sig.pow.db.nc
76	SAR_MLOOK_20170221200014_1_1_17.2G_VV_21_pres_16_fdc_166_249_332_415_498_581_665_748_831.sar.rgo.sig.pow.db.nc
77	SAR_MLOOK_20170221201129_1_1_17.2G_HH_12_pres_16_fdc_831_914_997_1080_1163_1246_1330_1413_1496.sar.rgo.sig.pow.db.nc

78	SAR_MLOOK_20170221201129_1_1_17.2G_HV_11_pres_16_fdc_831_914_997_1080_1163_1246_1330_1413_1496.sar.rgo.sig.pow.db.nc
79	SAR_MLOOK_20170221201129_1_1_17.2G_VH_22_pres_16_fdc_831_914_997_1080_1163_1246_1330_1413_1496.sar.rgo.sig.pow.db.nc
80	SAR_MLOOK_20170221201129_1_1_17.2G_VV_21_pres_16_fdc_831_914_997_1080_1163_1246_1330_1413_1496.sar.rgo.sig.pow.db.nc
81	SAR_MLOOK_20170221202338_1_1_17.2G_HH_12_pres_16_fdc_831_914_997_1080_1163_1246_1330_1413_1496.sar.rgo.sig.pow.db.nc
82	SAR_MLOOK_20170221202338_1_1_17.2G_HV_11_pres_16_fdc_831_914_997_1080_1163_1246_1330_1413_1496.sar.rgo.sig.pow.db.nc
83	SAR_MLOOK_20170221202338_1_1_17.2G_VH_22_pres_16_fdc_831_914_997_1080_1163_1246_1330_1413_1496.sar.rgo.sig.pow.db.nc
84	SAR_MLOOK_20170221202338_1_1_17.2G_VV_21_pres_16_fdc_831_914_997_1080_1163_1246_1330_1413_1496.sar.rgo.sig.pow.db.nc

#	*Feb 22, 2017 (X- and Ku-band)*
1	SAR_MLOOK_20170222154811_0_1_9.6G_HH_12_pres_8_fdc_390_488_585_683_781_878.sar.rgo.sig.pow.db.nc
2	SAR_MLOOK_20170222154811_0_1_9.6G_HV_11_pres_8_fdc_390_488_585_683_781_878.sar.rgo.sig.pow.db.nc
3	SAR_MLOOK_20170222154811_0_1_9.6G_VH_22_pres_8_fdc_390_488_585_683_781_878.sar.rgo.sig.pow.db.nc
4	SAR_MLOOK_20170222154811_0_1_9.6G_VV_21_pres_8_fdc_390_488_585_683_781_878.sar.rgo.sig.pow.db.nc
5	SAR_MLOOK_20170222154811_1_1_17.2G_HH_12_pres_8_fdc_-879_-782_-684_-586_-489_-391_-293_-196_-98.sar.rgo.sig.pow.db.nc
6	SAR_MLOOK_20170222154811_1_1_17.2G_HV_11_pres_8_fdc_-879_-782_-684_-586_-489_-391_-293_-196_-98.sar.rgo.sig.pow.db.nc
7	SAR_MLOOK_20170222154811_1_1_17.2G_VH_22_pres_8_fdc_-879_-782_-684_-586_-489_-391_-293_-196_-98.sar.rgo.sig.pow.db.nc
8	SAR_MLOOK_20170222154811_1_1_17.2G_VV_21_pres_8_fdc_-879_-782_-684_-586_-489_-391_-293_-196_-98.sar.rgo.sig.pow.db.nc
9	SAR_MLOOK_20170222163859_0_1_9.6G_HH_12_pres_8_fdc_878_976_1074_1171_1269_1367_1464_1562.sar.rgo.sig.pow.db.nc
10	SAR_MLOOK_20170222163859_0_1_9.6G_HV_11_pres_8_fdc_878_976_1074_1171_1269_1367_1464_1562.sar.rgo.sig.pow.db.nc
11	SAR_MLOOK_20170222163859_0_1_9.6G_VH_22_pres_8_fdc_878_976_1074_1171_1269_1367_1464_1562.sar.rgo.sig.pow.db.nc
12	SAR_MLOOK_20170222163859_0_1_9.6G_VV_21_pres_8_fdc_878_976_1074_1171_1269_1367_1464_1562.sar.rgo.sig.pow.db.nc
13	SAR_MLOOK_20170222163859_1_1_17.2G_HH_12_pres_8_fdc_97_195_292_390_488_585_683_781_878.sar.rgo.sig.pow.db.nc
14	SAR_MLOOK_20170222163859_1_1_17.2G_HV_11_pres_8_fdc_97_195_292_390_488_585_683_781_878.sar.rgo.sig.pow.db.nc
15	SAR_MLOOK_20170222163859_1_1_17.2G_VH_22_pres_8_fdc_97_195_292_390_488_585_683_781_878.sar.rgo.sig.pow.db.nc
16	SAR_MLOOK_20170222163859_1_1_17.2G_VV_21_pres_8_fdc_97_195_292_390_488_585_683_781_878.sar.rgo.sig.pow.db.nc